ISSN 0038-0946, Solar System Research, 2024, Vol. 58, No. 1, pp. 1–28. © The Author(s), 2024. This article is an open access publication.

Scientific Instrumentation Complex for the *ExoMars-2022* Landing Platform

O. I. Korablev[a], *, D. S. Rodionov[a], **, and L. M. Zelenyi[a], ***

[a] *Institute of Space Research, Russian Academy of Sciences (IKI RAS), Moscow, 117997 Russia*

**e-mail: korab@cosmos.ru*

***e-mail: rodionov@cosmos.ru*

****e-mail: lzelenyi@cosmos.ru*

Received August 17, 2023; revised September 5, 2023; accepted September 13, 2023

Abstract—Scientific objectives, instruments, and measurement program of the scientific instrumentation of the *Kazachok* stationary landing platform of the State Corporation Roscosmos and the European Space Agency (ESA) ExoMars-2022 project are presented. The scientific objectives of research on the landing platform included the long-term climate monitoring, the studies of the atmospheric composition, the mechanisms for dust lifting and related electrical phenomena, atmosphere–surface interactions, the subsurface water abundance, monitoring the radiation situation, and the study of Mars internal structure. To address these problems, 11 Russian and two European instruments with a total mass of 45 kg were built, tested and integrated into the spacecraft. These include a television camera system, meteorological complexes, a suite for studying dust and related electrical phenomena, optical spectrometers and an analytical complex for studying the atmospheric composition, a microwave radiometer, the neutron and gamma spectrometers for surface research, a seismometer, magnetometers and a Mars proper motion experiment to study its internal structure. Although the ExoMars-2022 project has been discontinued, the scientific objectives of the landing platform have not lost their relevance, and the technical solutions and developments implemented in scientific equipment are of interest and promising for further Mars exploration.

Keywords: Mars, space research instruments, atmosphere, dust, surface, magnetic field, internal structure, meteorology, dosimetry

DOI: 10.1134/S0038094624010064

INTRODUCTION

Recent issues of the *Solar System Research* journal began the publication of a series of articles devoted to experiments prepared for the *Kazachok* landing platform (Moskatinyev et al., 2020a; 2020b) of the ExoMars-2022 project of the State Corporation Roscosmos and the European Space Agency (ESA) (Vago et al., 2015a). The launch of an automatic interplanetary station, consisting of a European cruise module, a Russian descent module with a landing platform (LP) and the European rover, was scheduled for September 2022 from the Baikonur Cosmodrome using a Proton-M launch vehicle with a Briz-M upper stage.

The landing was scheduled to take place in 2024 in the Oxia Planum region located near the equator in the northern hemisphere of Mars, east of the Chryse Planitia, on the border of highland and lowlands (Vago et al., 2015b; Ivanov et al., 2020). The landing area is a 120×19 km ellipse inside a shallow crater. Here phyllosilicates (clay rocks) enriched in iron and magnesium come to the surface. Above them there lies a layer of a dark material, possibly of volcanic origin, which has been eroded over the past 100 million years. The latter is not known to have undergone temperature-related changes or metamorphism. There are no significant elevations inside the ellipse of landing, and it offers a fairly flat terrain for landing.

For reasons unrelated to scientific or technical problems, the international cooperation ExoMars was terminated in the spring of 2022 and the launch did not take place. At the same time, the scientific equipment was fully prepared, tested and integrated on the LP. The scientific objectives of the complex have not lost their relevance, and the technical solutions and developments implemented in the scientific instruments are of interest and promising for further research of Mars.

Scientific objectives of the scientific instrumentation complex (SIC) and its composition, corresponding to the early stage of the project (before 2014), were presented in (Zelenyi et al., 2015). Since then, the scientific objectives and composition of SIC have undergone significant changes. First of all, it was decided to renounce taking soil samples with a help of a manipulator arm and their analysis with an onboard analytical

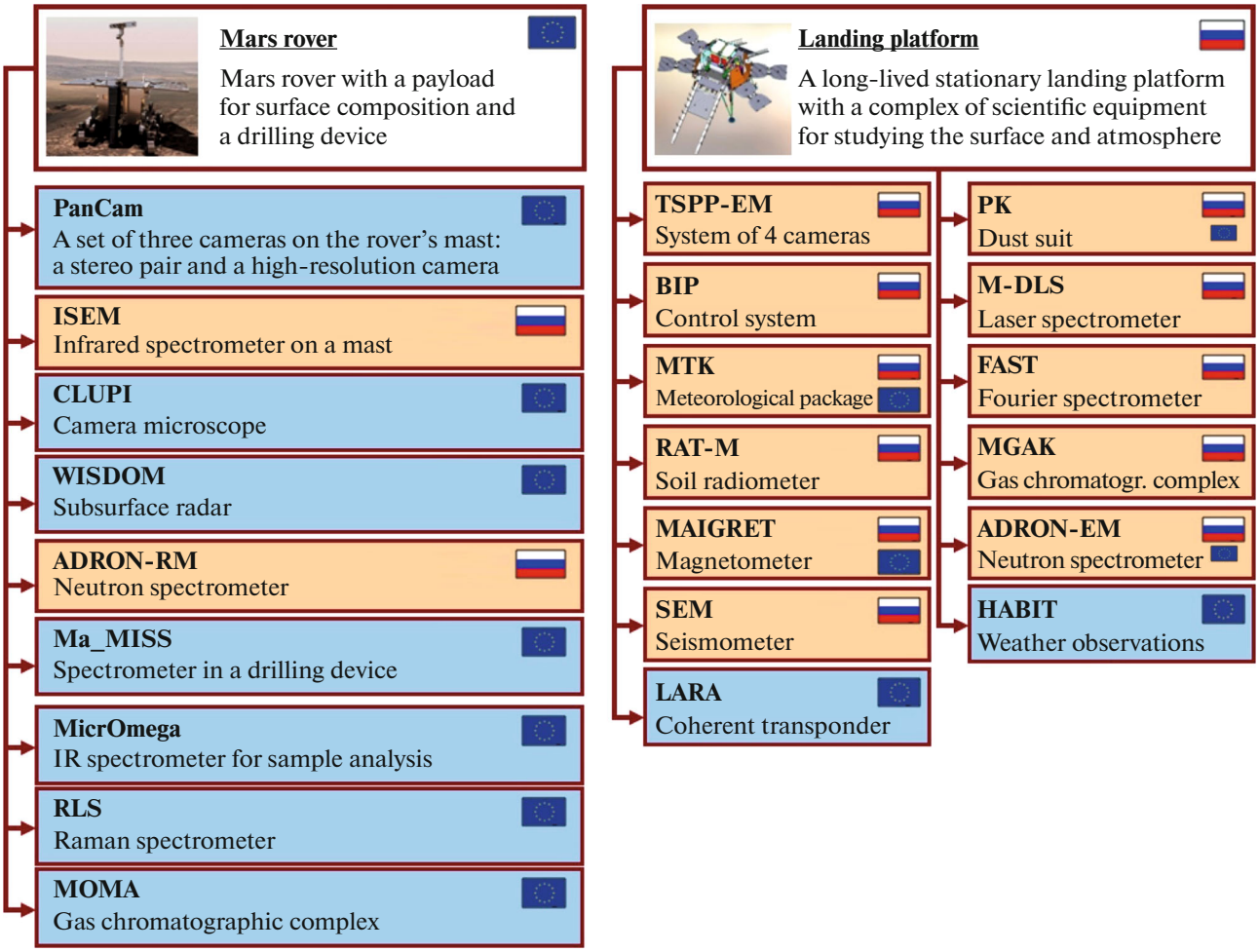

Fig. 1. Scientific instruments of the Rosalind Franklin rover and the *Kazachok* landing platform.

laboratory based on a gas chromatograph and mass spectrometer. This task would be most optimally accomplished from a mobile platform, the Rosalind Franklin rover (Vago et al., 2017). In addition, SIC was supplemented by a number of European instruments and sensors, selected following an international competition that ended in November 2015. Two European instruments (LaRa and HABIT) were selected; some European blocks and sensors were incorporated into Russian instruments (MAIGRET, MTK and PK). Thus, the mutual participation of international cooperation partners in two segments of the project was balanced: the Rosalind Franklin rover with predominantly European scientific equipment and the *Kazachok* LP with predominantly Russian equipment. The composition of scientific equipment of the rover and LP is shown in Fig. 1. A photograph of the LP with the installed rover during the assembly process is given in Fig. 2. The SIC instruments are mainly located at the level of the LP deck to the right and left of the rover.

The purpose of the series of publications and this paper is to present the SIC state based on the completion of the LP development and testing in 2022. The SIC included 13 instruments (36 blocks), with a total mass (including the cable system) of ≤45 kg.

By the time this paper has been prepared, seven articles devoted to the LP SIC instruments and sensors were published in the *Solar System Research* (2022–2023). Another six papers adequately describing the SIC instruments were published in other journals (relevant references are given in Table 2). Unfortunately, up-to-date and detailed descriptions of three instruments and the main SIC meteorological package are not yet available. We hope that they will appear in the near future, and this paper will be able to partially compensate for the lack of information.

The research tasks of SIC are discussed in the section SCIENTIFIC TASKS, the brief information about instruments of the complex is collected in the section SCIENTIFIC EXPERIMENTS ON LANDING PLATFORM, examples of measurement scenar-

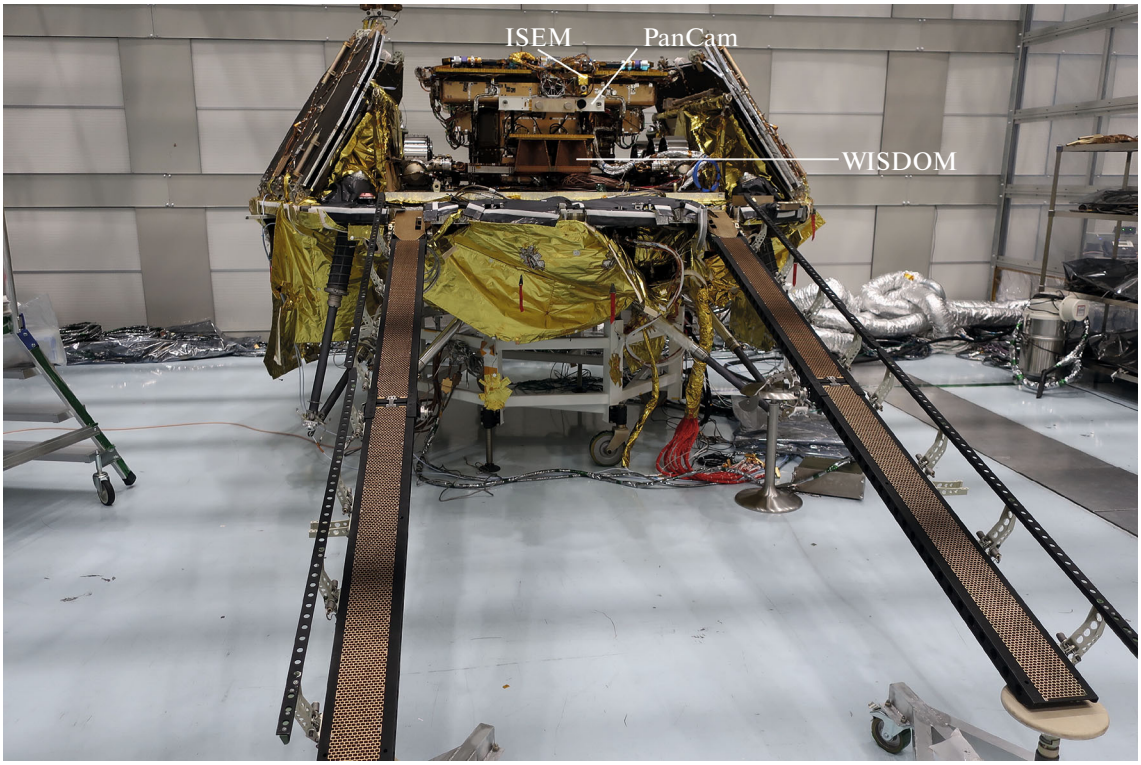

Fig. 2. Landing platform and rover under assembly at the TAS-I enterprise (Turin, Italy). The optical units of the PanCam and ISEM instruments and the WISDOM radar antenna of the rover are marked. Photo by IKI RAS.

ios are given in the section SCIENCE OPERATIONS PLAN.

SCIENTIFIC TASKS

Immobile landing platforms have been repeatedly and successfully used in the history of Mars exploration: NASA's projects *Viking-1*, *Viking-2*, *Pathfinder*, *Phoenix*, and *InSight*. Before the advent of mobile platforms, they targeted primarily research and, to a lesser extent, monitoring goals (Viking, Phoenix). In recent years, the emphasis has shifted to monitoring (*InSight*). A fixed platform is undoubtedly the best option for meteorological and geophysical monitoring. It is also expedient to solve a number of important research problems related to studies of the atmosphere and atmosphere-surface interactions on a fixed platform. Combining the objectives of surface and atmospheric research, even using the most advanced equipment, leads to inevitable compromises when planning experiments, reducing the priority of atmospheric research. At the same time, in studying the surface composition, habitability, search for signs of life remotely or by collecting and analyzing soil samples, mobility, the ability to choose the location for analyses, is a key advantage. These considerations were taken into account when formulating the scientific tasks and selecting the scientific instrumentation for the *Kazachok* LP and sharing tasks between the LP and the Rosalind Franklin rover.

When planning the mission, (Zelenyi et al., 2015) declared the following scientific tasks of the LP: (1) long-term monitoring of climatic conditions on the Mars surface at the landing site; (2) study the composition of the Martian atmosphere from the surface; (3) study the interaction of atmosphere and surface; (4) study the surface composition; (5) study the internal structure of Mars; (6) monitoring of the radiation situation and other factors. Taking into account the mentioned changes in emphasis, the scientific objectives of research on the landing platform by the time it was ready can be formulated as follows:

1. Long-term climate monitoring.

2. Atmosphere composition research.

3. Study of dust lifting mechanisms and related electrical phenomena.

4. Investigation of surface–atmosphere interactions.

5. Study of the abundance of water in the subsurface.

6. Monitoring of the radiation environment.

7. Study of the internal structure of Mars.

The list of scientific experiments and their correspondence to scientific objectives is given in Table 1.

Table 1. Correspondence of scientific tasks of the *ExoMars* LP and scientific experiments

Instruments	Scientific objectives						
	Climate monitoring	Atmosphere composition	Dust and atmosphere electricity	Atmosphere/surface	Subsurface water	Radiation environment	Internal structure
TSPP-EM (Television system)	×		×	×			
MTK (Meteorological package)	●	×	×	×			
HABIT (Instrument package for investigating the amount of water vapor in the atmosphere, daily and seasonal variations in ground and air temperatures)	●	×	×	×			
PK (Dust suit)	×		●	×			
FAST (Fourier spectrometer)	×	●	×	×			
MGAK (Gas analyzer package)		●		×			
M-DLS (Laser spectrometer)		×		●			
RAT-M (Radiometer)	×		×	●	×		
ADRON-EM (Neutron and gamma spectrometer with activation; dosimeter)				×	●	×	
MAIGRET, ARM (Magnetometers)			×		×		●
SEM (Seismometer)							●
LARA (Radio beacon)							●

● indicates the primary scientific objective, × indicate additional scientific goals.

The order of experiments in the table approximately reflects their compliance with the scientific objectives.

Scientific Objectives Related to the Atmosphere

Long-term climate monitoring, studying atmospheric composition and atmospheric dust phenomena are the key and closely related scientific themes of the *ExoMars* LP. They break down into the following major components: (1) regular long-term hourly monitoring of the main meteorological parameters (temperature, pressure, wind speed and direction, and humidity), providing a basis for tuning and validating Mars atmospheric general circulation models; (2) regular measurements of atmospheric gases, including noble gases, and their isotopologues to determine the daily and seasonal dynamics of the atmosphere composition near the Martian surface and surface–atmosphere interactions, elucidating the isotopic ratios of volatile compounds in various reservoirs; (3) studying the atmospheric structure and the dynamics of planetary boundary layer during the descent of the landing module and remotely from the surface; study of the dynamics of the near-surface atmospheric layer; (4) study of dust lifting mechanisms and transport processes, including measurements of the momentum of near-surface dust particles simultaneously with their sizes and recording of related electrical phenomena.

There have been relatively few full-fledged weather stations on numerous vehicles that reached the surface of Mars: *Viking Lander* (VL) *-1*, *-2* (Chamberlain et al., 1976), *Phoenix* (Taylor et al., 2008); the *Curiosity* and *Perseverance* rovers (Gómez-Elvira et al., 2012; Rodriguez-Manfredi et al., 2021) and the Interior Exploration using Seismic Investigations, Geodesy and Heat Transport (*InSight*) platform (Spiga et al., 2018). Elements of weather stations were also present on *Mars Pathfinder* and the *Zhurong* rover (Seiff et al., 1997; Liu et al., 2022). Of particular value are long series of observations and, until recently, the pressure records from VL-1, -2 (Hess et al., 1980) were main means of calibrating the models of general circulation of Martian atmosphere. Richly equipped with a variety of weather sensors, with a high degree of redundancy, the

Table 2. Scientific instruments of SIC of *ExoMars-2022* LP

Instrument/ Subsystem	Principle of operation	Basic measurements	Principal Investigator, Manufacturer	Weight/ dimensions/ consumption/ information capability	Reference
TSPP	Four color cameras, field of view of each is 115°×115°	Panorama of the surface, variable phenomena	I.V. Polyanskiy (IKI, RAS)	Four cameras and electronics unit 5.3 kg, 12.5 W	Abramov et al. (2023)
MTK (METEO)	Meteorological sensors, optical density sensors, accelerometer, lidar	Monitoring of basic atmospheric parameters, measurements on the descent (see Table 3)	O.I. Korablev (IKI RAS), Finland, Spain	Seven blocks 5.2 kg	See Table 3
HABIT	Sensors of temperature, atmosphere, surface, and UV radiation	Assessment of the possibility of formation of liquid brines, the surface habitability	J. Martin-Torres Sweden	Two blocks 0.8 kg	Martín-Torres et al. (2020)
PK (Dust suit)	Impact dust sensors, nephelometer, electric field sensors	Properties of dust at the surface, dust lifting, its electrification	A.V. Zakharov (IKI RAS), Italy, France	Two blocks of 0.8 and 0.5 kg; boom 0.3 kg 10 W 4 Mb/sol	Zakharov et al. (2022)
FAST	Fourier spectrometer, analysis of atmosphere's self-radiation and the solar spectrum through the atmosphere (1.7–17 μm)	Atmospheric composition, planetary boundary layer	A.V. Shakun (IKI RAS)	3.4 kg	Shakun et al. (2017)
MGAK	Analysis of atmospheric samples with a gas chromatograph and mass spectrometer	Atmospheric composition, including noble gases	M.V. Gerasimov (IKI RAS)	Two blocks 6.9 kg	Gerasimov et al. (2014)
M-DLS	Analysis of atmospheric samples with a laser spectrometer	Daily and seasonal cycle of water vapor, CO_2, and their isotopes	A.V. Rodin (MIPT, IKI RAS)	3 kg 35 × 19 × 11 cm^3 10–12 W 0.5 Mb/sol	Rodin et al. (2020)
RAT-M	Microwave radiometer in three bands (6–15 GHz)	Soil temperature to a depth of 1 m	D.P. Skulachev (IKI RAS)	0.6 kg 9.5 × 9.5 × 3 cm^3 + antennas 2.5 W 0.01 Mb/sol	–

Table 2. (Contd.)

Instrument/ Subsystem	Principle of operation	Basic measurements	Principal Investigator, Manufacturer	Weight/ dimensions/ consumption/ information capability	Reference
ADRON-EM	Neutron and gamma spectrometer with activation by neutron pulses, the dosimeter	Surface hydration monitoring. Content of rock-forming and radiogenic elements. Accumulated dose monitoring	I.G. Mitrofanov (IKI RAS), Bulgaria	Three blocks 5.9 kg	Mokrousov et al. (2022)
MAIGRET	Fluxgate magnetometer (100 Hz–20 kHz)	Magnetic field intensity and direction	A.V. Skalsky (IKI RAS), Czechia	Three blocks 2.9 kg	Kolmasova et al. (2017)
AMR	Magnetoresistive sensor on the retractable boom	Magnetic field intensity and direction	M. Díaz Michelena, Spain	0.35 kg	Díaz Michelena et al. (2023)
SEM	Triaxial seismometer	Transverse and longitudinal surface oscillation	A.B. Manukin (IFZ RAS, IKI RAS)	6 kg $25 \times 25 \times 35$ cm^3 3.5 W 1 Mb/sol	Manukin et al. (2021)
LaRa	Coherent X-band transponder	Precession and nutation of Mars	V. Dehant, Belgium	2.15 kg $25 \times 8 \times 8$ cm^3 + antennas 42 W 0 Mb/sol	Dehant et al. (2020)
BIP	Unit of interfaces and memory	Instrument control and acquisition of scientific information	K.V. Anufreychik (IKI RAS)	2.5 kg $22 \times 19 \times 6.6$ cm^3 9 W <80 Mb/sol	–

ExoMars LP would provide a worthy contribution to the study of Martian meteorology.

Regular measurements of minor and abundant constituents of the Martian atmosphere and their isotopologues provide insight into the details of the major climate cycles of Mars: carbon dioxide, dust and water. Up to 30% of the main component of the atmosphere (CO_2) condenses on the polar ice caps in winter, causing corresponding variations in pressure and changes in the mixing ratio of noncondensable components (Ar, N_2, CO). Water, present in trace amounts in the Martian atmosphere, nevertheless, plays a key role in chemical transformations preventing the photolytic break down of CO_2, forms condensation clouds that regulate atmospheric heating, and, over longer timescales, supports the migration of glaciers across the surface of Mars (Montmessin et al., 2017). Adsorption and desorption of water in the top soil layer is a poorly understood process, apparently playing the role of friction in the water cycle (Jakosky et al., 1997; Navarro et al., 2014). Orbiters around Mars—*Mars Express* (MEx), *Mars Reconnaissance Orbiter* (MRO), *ExoMars Trace Gas Orbiter* (TGO)—regularly monitor the major and well-known minor components (CO_2, CO, H_2O, O_3) by remote methods (see, e.g., Smith et al., 2017; 2021; Knutsen et al., 2022; Lefèvre et al., 2021). Measurements on the surface using the spectroscopic and gas analytical equipment (M-DLS, MGAK, ozone sensors SIS, HABIT) would make it possible to reliably tie the remote measurements to the surface and estimate the time scales of daily and seasonal atmosphere–surface interactions.

Measuring the isotopic ratios of hydrogen, oxygen and carbon in water vapor and CO_2 during the atmosphere–surface exchange would allow, in addition to refining their values, known mainly from remote sensing results (e.g., Alday et al., 2021a; 2021b) and from single measurements at the surface (Webster et al., 2013), to identify differences between atmospheric and surface volatile reservoirs. Finally, measurements of noble gases and their isotopes are very high priority: they can be used to infer the distant history of the atmosphere and volatiles on Mars, while their surface measurements have only been carried out by the *Curiosity* rover or *Mars Science Laboratory* (MSL) (Mahaffy et al., 2013; Wong et al., 2013; Atreya et al., 2013; Conrad et al., 2016).

Studying the atmosphere during the descent of the landing module is a necessary task of the project. It is closely related to the technical problems of the descent capsule entering the atmosphere and the descent of the landing module. Density values for the upper atmosphere can vary many-fold from models, and it is not surprising that more than two-thirds of landings on Mars have failed. We know 11 atmospheric profiles measured during descent: *Mars-6* (Avduevsky et al., 1975); *VL-1*, *-2* (Seiff and Kirk, 1977); *Mars Pathfinder* (Magalhães et al., 1999); Mars Exploration Rovers (MER) *Opportunity* and *Spirit* (Withers and Smith, 2006); *Phoenix* (Blanchard and Desai, 2011); *Mars Science Laboratory* (MSL) (Holstein-Rathlou et al., 2016); *ExoMars-2016 Schiaparelli* (Aboudan et al., 2018); InSight (Karlgaard et al., 2021) and *Perseverance* (Karlgaard et al., 2023). To reconstruct the descent profile, the ExoMars-2022 project included measurements of the deceleration of the descent capsule using data from the spacecraft's inertial unit, the AMELIA experiment (Ferri et al., 2019), and with MTK accelerometers. The atmospheric density is measured, from which a pressure and temperature can be obtained in a hydrostatic approximation. Horizontal wind speed can also be obtained from accelerometer data. After the parachute is deployed, temperature and pressure measurements were planned using MTK sensors.

Monitoring and study of the planetary boundary layer (PBL) is also one of the tasks of high importance for the further Mars exploration and prospective manned expeditions (Petrosyan et al., 2011; Read et al., 2017). The atmosphere dynamics in the near-surface layer is closely related to the following problem: wind measurements and understanding of mechanisms that determine near-surface winds underlie the study of dust lifting and transport, and the initiation of large-scale dust events. The state of the PBL in specific locations is already well described by mesoscale dynamic models (see, e.g., (Toigo et al., 2002)). For boundary layer studies, the MTK and PK data are of crucial significance. These instruments, as well as a system of cameras, will help to track another specific element of the Martian climate—local vortices or dust devils (see, e.g., (Kurgansky, 2022))—involved in the dust lifting (Neakrase et al., 2016), and likely generating strong electric fields and discharges (Renno et al., 2003). Dust storm on the Earth produces electric fields of ~100 kV/m. Similar fields on Mars would exceed the breakdown voltage (~20 kV/m), so one should expect discharges likely having a strong influence on chemical transformations in the atmosphere and even surface habitability (Atreya et al., 2006; Kok and Renno, 2009). These discharges could be recorded by MAIGRET and PK. During exploration of Mars by landers and rovers, a detailed description of the near-surface atmospheric profile has been obtained only once using the Mini-TES/Mars Exploration Rovers (MER) Fourier spectrometer (Smith et al., 2006). The FAST experiment would allow these data to be obtained regularly, complementing the MTK and PK studies.

As already mentioned, the dust cycle belongs to the main atmospheric cycles of Mars (Kahre et al., 2017). Unlike Earth, where the heat balance of the atmosphere and, eventually, the surface is determined predominantly by gas absorption (water vapor), dust plays this role in the thin atmosphere of Mars. It absorbs the incoming solar radiation in the visible range and traps the thermal radiation leaving the planet (in the silicate

9-μm absorption band). A modern model of the optical properties of dust particles, based mainly on remote observations, is given by (Wolff et al., 2009). The hotter summer in the southern hemisphere, when Mars is closer to the Sun, increases the circulation and dust load in the atmosphere, warms it up, in turn increasing the dust uplift (Daerden et al., 2015). This positive feedback periodically, on average once every three Martian years, leads to global dust storms (GDSs) covering almost all tropical and midlatitudes (see, e.g., (Guzewich et al., 2020)). Historically, general circulation models describing the climate of Mars have used available measurements of atmospheric dust (Forget et al., 1999; Hartogh et al., 2005; Wilson and Hamilton, 1996). Upon the availability of regular observations from orbiters and landers, total dust optical depths, and vertical dust profiles (Montabone et al. 2015), the Martian Climate Database (MCD) fairly well reproduces atmospheric conditions during a given Martian year or for some typical scenarios. Another class of models attempts to parameterize the processes of dust lifting from the surface and describe its transport by circulation flows (Kahre et al., 2023; Neary and Daerden, 2018; Newman and Richardson, 2015). Parameterizations are based mainly on theoretical concepts and measurements in wind tunnels that simulate conditions on Mars (see, e.g., Martin and Kok, 2017; Sagan and Bagnold, 1975), including even the gravity (Musiolik et al., 2018). Although this issue receives much attention, direct data on saltation, transport, electrification of dust and discharges under real conditions on Mars are almost absent. The lack of understanding of dust uplift and transfer near the surface means that self-consistent models are not yet able to reproduce the conditions for the occurrence of GDS. The joint work of PK and MTK would for the first time make it possible to study comprehensively the processes of dust lifting from the surface of Mars. Additional information on dust phenomena and dust properties could be obtained from observations with TSPP cameras, from MAIGRET electromagnetic field monitoring, and by combining infrared FAST data with orbital measurements (Wolff et al., 2006).

Atmosphere–Surface Interaction Studies

The study of interactions between the atmosphere and the surface is closely related to the atmospheric objectives and is adjacent to surface studies. Such interactions include the already mentioned mechanisms of dust lifting, its reverse impact on the surface and the study of the atmospheric boundary layer. In such studies, the main role would be played by the experiments of MTK, PK, and TSPP.

Another line of research targeted monitoring the exchange cycles of volatile components between the atmosphere and the surface. In particular, by measuring the H_2O content and the isotope ratios D/H, $^{18}O/^{17}O/^{16}O$, $^{13}C/^{12}C$ in H_2O and CO_2 near the surface at different times of day during the seasonal cycle, it is possible not only to clarify the physical and chemical processes occurring between the surface and the atmosphere, but also to draw conclusions about the habitability of Mars in the past and present (see, e.g., Franz et al., 2020). The leading role in these studies was given to the M-DLS laser spectrometer and the MGAK analytical package. Atmospheric humidity and topsoil hydration could be assessed by the MTK humidity sensor and the ADRON-EM instrument, respectively. Auxiliary information about physical conditions in the atmosphere, on the surface and in the upper layer of soil could be obtained by the MTK and HABIT sensors, the FAST IR spectrometer and the RAT-M microwave radiometer.

Study of the Abundance of Water in the Surface Layer

Water in the near-surface layer of Martian soil can be in the form of ice, adsorbed by regolith granules, or bounded within minerals. The presence of water near the landing site may testify both to the prospects of the location in terms of habitability and the further exploration by space means, and to the geological past of the planet: hydrated minerals could have formed in liquid water reservoirs of early Mars. The information on water distribution can be obtained from radar sounding data, but outside the polar ice caps, in low and middle latitudes, the neutron monitoring data serve as a main source. Long-term orbital measurements of the neutron flux induced by cosmic radiation showed the presence of hydrogen nuclei in the upper (1–2 m) layers of regolith, corresponding to a mass fraction of water from units of percent to 20–40% (see, e.g., Malakhov et al., 2022). To detect ice at equatorial latitudes is possible only in deep canyons (Mitrofanov et al., 2022a). According to data of neutron logging activated using a neutron pulse generator at MSL, the mass fraction of water along the rover path was from ≤0.5 to ≥6% (Mitrofanov et al., 2022b).

From the ExoMars LP, it was planned to measure the hydration of the surface of Mars to a depth of 1–2 m using the ADRON-EM neutron detector. During the first few days after landing, the instrument was supposed to work together with ADRON-RM (Mitrofanov et al., 2017) and geophysical radar WISDOM (Ciarletti et al., 2017) on the *Rosalind Franklin* rover. As the rover moves away from the platform, these measurements would provide the priority information on the vertical distribution of water in all its forms. The influence of temperature changes on the vertical distribution of water was supposed to be clarified using estimates of the daily and seasonal temperature variations at three levels (up to ~1 m) below the surface using the RAT-M radiometer.

The ADRON-EM device was also supposed to provide the information on the elemental composition of the main rock-forming and radiogenic elements in the immediate vicinity of the landing site. At the same

time, the density of the soil is measured. Thus, the ADRON-EM experiment could fulfill the scientific task formulated for the original configuration of the SIC: studying the surface composition. Additional data on the nature of rocks near the lander can be obtained from estimates of soil electrical conductivity using MAIGRET and AMR magnetometers.

Monitoring of Radiation Environment

The radiation environment on the surface of Mars, both now and in the past, is critical for the habitability and ability to sustain life on the planet. It affects any potential life forms that could survive underground (see, e.g., Pavlov et al., 2010). High-energy radiation and the associated risks to human health largely determine planning for future manned missions to Mars.

Mars (its upper atmosphere) interacts with two types of high-energy radiation: galactic cosmic rays (GCRs) and energetic solar-wind particles. The monitoring of these radiations in orbit around Mars is performed by the Liulin-MO dosimeter within the FREND/TGO instrument (Mitrofanov et al., 2018; Semkova et al., 2021). Due to the thin atmosphere, GCRs and solar wind particles reach the surface, where they produce secondary particles, including neutrons and gamma rays. Secondary particles are also formed as a result of interaction with the atmosphere. Thus, the surface radiation environment differs significantly from the situation in orbit. The first and the only direct measurements of radiation on the surface of Mars were made with the RAD instrument on *Curiosity* (Hassler et al., 2012; 2014; Ehresmann et al., 2023). On the *ExoMars* landing platform, monitoring of the radiation environment was planned using the Lulin-ML dosimetric channel of the ADRON-EM and the neutron and gamma-ray detectors of the ADRON-EM instrument itself.

Studying the Internal Structure of Mars

The study of the internal structure of Mars is directly related to the fundamental problem of the formation and early evolution of the Solar System planets. Refinement of models of the internal structure allows the estimation of a proportion of volatile components collected by the planet during the early stages of accretion and intense bombardment (Zharkov, 1996). From the viewpoint of analogies between Earth and Mars, the processes of differentiation and further evolution of the interior are no less important. Mars is the only planet similar to Earth, which can be studied for a long time by geophysical methods, and fixed stations on its surface, preferably several, are the optimal platform for these studies (see, e.g., Lognonné et al., 2000).

The main method for studying the internal structure is seismometry. Carrying out such measurements on the surface of another planet is a complex technical task. In addition to a high sensitivity and a wide frequency range, a seismometer on Mars must be protected from wind, fluctuations of temperature and pressure, and isolated from the influence of the platform itself. After the mixed results of the seismic experiments of the *Viking Landers* (1976–1982) (Anderson et al., 1976) and the *Mars-96* attempt (Linkin et al., 1998; Lognonné et al., 1998), it took more than 20 years to implement the dedicated platform *InSight* (2018–2022). The SEIS vacuum seismometer, deployed on the surface separately from the *InSight* lander and heavily shielded from atmospheric influences (Lognonné et al., 2019), has recorded several significant seismic events and many minor ones (see, e.g., Giardini et al., 2020; Kawamura and al., 2023). A rich material was obtained on the thickness and properties (Knapmeyer-Endrun et al., 2021), the mantle properties (Huang et al., 2022), and a response from the core was gained (Stähler et al., 2021).

Studies of the Mars could be expanded using an additional geophysical station (see, e.g., Gudkova et al., 2014). Recording of seismic events simultaneously from two points on the surface would allow one to obtain the important information about the heterogeneity of the crust and mantle and to progress from profiles to a 3D structure, which can be reconstructed in an area comparable to a distance between stations. In this case, it is permissible to use an instrument even with more modest parameters than SEIS/*InSight*. This was the task assigned to the SEM seismometer of *ExoMars* LP, the launch of which was initially planned in 2018, simultaneously with *InSight*.

Analysis of the Doppler shift during two-way radio communication between a lander on Mars and ground stations allows one to determine parameters of the orientation and rotation of Mars, which makes it possible to refine the information about the internal structure, particularly the core. The target parameters are variations in rotation rate (or length of the day) and rotation axis orientation (precession and nutation). Previously, these experiments were carried out on the *Viking* (Yoder and Standish, 1997) and Mars *Pathfinder* (Folkner et al., 1997) landing modules. Attempts to constrain orbital parameters have also been made using Doppler tracking of orbiters and rovers (Kuchynka et al., 2014; Konopliv et al., 2016; 2020). The LaRa experiment, a coherent X-band transponder, was designed to track the position of the lander with high accuracy (Dehant et al., 2020; Le Maistre et al., 2020; Péters et al., 2020).

The magnetic field is associated with the internal structure of the planet, and with the evolution of its atmosphere. The remnant magnetization of Martian crust, an evidence of the ancient magnetic field, was first mapped by *Mars Global Surveyor* (MGS) from a 400-km orbit (Acuña et al., 1999) and complemented by measurements from the elliptical MAVEN orbit (Connerney et al., 2015). Models allow the magnitude of magnetic field to be extrapolated to the surface (see,

e.g., Langlais et al., 2019). To date, measurements of the surface magnetic field have been carried out on the *InSight* lander (Johnson et al., 2020) and the *Zhurong* rover (Liu et al., 2022). The field measured at the *InSight* landing site appeared to be an order of magnitude stronger than was predicted by the satellite model (Johnson et al. 2020). Crustal magnetic fields interact with the solar wind, to create transient fields and currents in the upper atmosphere of Mars. At the surface, diurnal variations, a result of ionospheric currents, and higher frequency changes, still remaining to be explained, have been observed (Mittelholz et al., 2020). More data on the surface magnetic field are needed to explain the nature of these effects and the ancient dynamo. In addition, alternating fields, in combination with geomorphological and seismic data, can be used to study the electrical conductivity of the Martian interior. Measurements of the magnetic field strength and direction at the ExoMars landing site were planned using the MAIGRET and AMR magnetometers.

SCIENTIFIC EXPERIMENTS OF THE LANDING PLATFORM

The list of scientific instruments of the *ExoMars* LP is given in Table 2. Their order corresponds to Table 1.

TSPP-EM Television System of the ExoMars Landing Platform

The TSPP-EM system of cameras includes five units, four KAM-O/EM cameras and an electronics block for collecting, storing and processing information BSD/EM (Abramov et al., 2023). The instrument was manufactured at IKI RAS. The cameras are installed at the corners of the landing platform at a height of about 1 m. In the azimuthal plane, their optical axes are spaced 90° apart, and their fields of view (115°×115°) overlap, which allows for a complete overview of the horizon line. Starting from a distance of several meters, a full circular panorama of the landing site around the LP is formed. It was planned to construct a video series of images, in particular, filming during the landing process, filming the rover's egress from the LP, or recording the fast-flowing phenomena such as dust devils.

The maximum resolution of camera photodetectors is 2048 × 2048 pixels with the possibility of framing (2048 × 512) and binning (2 × 2) to reduce the amount of transmitted information. The bit depth of the resulting images is 14 or 12 bits. Images can be obtained in color at three wavelengths: 450, 550 and 650 nm (RGB) or in panchromatic mode. The depth of field is from 1 m to infinity. The cameras are of measurement quality in terms of both photometric and angular characteristics.

The main scientific objectives to be adressed by TSPP-EM can be formulated as follows: in relation to the surface of Mars, it is the geomorphological analysis of the terrain around the landing site using panoramas obtained on the surface and in the final sections of the descent of the landing module. The mineralogical analysis of surface areas is performed through measurement of spectral brightness (chromaticity). Regarding the atmosphere of Mars, it is the analysis of the properties of atmospheric aerosol, based on observations of the angular distribution of sky brightness, with the ability to separate the dust and condensation components. Observations of dust transport over the surface to understand the saltation processes. Filming dust devils and the assessment of their characteristics, sizes, and velocity. Atmospheric observations by TSPP-EM would complement and expand the research in the MTK and PK experiments.

The most important task of TSPP-EM is the information and engineering support of the entire project. It is hard to imagine landing on the surface of Mars without the ability to obtain visual images.

Meteorological Packages MTK and HABIT

The main meteorological package of the landing platform, MTK (or METEO), consists of two parts: a set of sensors for measurements mainly during the descent of the landing module (MTK-L) and the meteorological package proper with temperature, pressure, wind, humidity, dust, illumination sensors for measurements on the surface, many of which are placed on a meteorological boom (METEO Boom). Each part has its own control and data acquisition system. In addition, to optimize the control of small units, elements not directly related to meteorology, a microphone for recording the sounds of Mars, and an AMR magnetic field sensor were included in the MTK. As a result, the MTK is a complicated package of many sensors and subsystems, for a total of 12 blocks, with international participation. IKI RAS was responsible for the integration and testing of the package.

The HABIT (HabitAbility: Brine Irradiation and Temperature) instrument was part of the European payload of the LP. Consisting of three blocks, it was developed and manufactured by the Swedish company Omnisys and the Luleå University of Technology. Although the main goal of the experiment was formulated as an assessment of the current habitability of the landing site (Martín-Torres et al., 2020), the basis of the instrument is sensors, partially overlapping with the MTK. The sensor and unit composition of the MTK and HABIT is detailed in Table 3.

During the descent of the lander, at first accelerometers operate to measure the deceleration of the descent capsule (Lipatov et al., 2023a). The deceleration is directly related to the atmospheric density, from which a pressure and temperature can then be calcu-

Table 3. Sensors and subsystems of MTK and HABIT instruments

Subsystem	Principle of operation	Designation	Manufacturer	Reference
MTK-L	Three blocks	Measurements during the descent and on the surface	IKI RAS	
BD	Triaxial accelerometer	Measurement of deceleration and angular velocity of the descent module. Restoring atmospheric density before the aerodynamic shield jettisoned	IKI RAS	Lipatov et al. (2023a)
BD	Membrane-type sensor of pressure	Pressure measurement (10^{-4}–12 mbar) during the descent and on the surface	IKI RAS	Lipatov et al. (2023b)
	Sensor of temperature, thermal resistance	Temperature measurement (±0.1°C, rel. accuracy of 0.01°C) during the descent and on the surface	IKI RAS	Lipatov et al. (2023b)
BDA	Lidar	Surface aerosol profile measurement (0–5 km)	IKI RAS	Lipatov et al. (2023c)
BDVA		Control and data acquisition unit of MTK-L	IKI RAS	
METEO Boom of MTK		Deployment of meteorological sensors at a height of up to 1 m above the LP. Surface measurements	IKI RAS	–
Three temperature sensors	Thermal resistances and thermocouples at three levels (125, 150, 175 cm from the surface)	Monitoring of atmospheric temperature (±0.2 °C, rel. accuracy of 0.01°C)	IKI RAS	Lipatov et al. (2023b)
Wind sensor	Ionization anemometer on the METEO Boom	Measuring the wind speed and direction	IKI RAS	Evlanov et al. (2015)
Solar irradiance sensor SIS'2022	Measuring the intensity of solar radiation in the range of 0.2–1 μm (on the METEO Boom)	Assessment of UV radiation, ozone content, optical density of the atmosphere	INTA (Spain)	Jimenez-Martín et al. (2023)
Humidity sensor METEO-H	Humicap® sensor (on the METEO Boom)	Humidity measurement	FMI (Finland)	–
Pressure sensor METEO-P	Barocap® sensor (in the control block MTK BU)	Monitoring of pressure	FMI (Finland)	–
Optical dust sensor ODS	Light measurement during the day at two wavelengths (masked photodiodes)	Measuring optical density of the atmosphere	IKI RAS	Khorkin et al. (2023)
Dust sensor DS'20	IR nephelometer (2.3 μm)	Estimation of large dust particles concentration near the surface	INTA (Spain)	–
Microphone*		Recording sounds of Mars	IKI RAS	–
Magnetometer AMR*	Magnetoresistive sensor at a distance of 2 m from the LP	Magnetic field measurements, including during the descent stage	INTA (Spain)	Díaz Michelena et al. (2023)

Table 3. (Contd.)

Subsystem	Principle of operation	Designation	Manufacturer	Reference
BU MTK		Control and data acquisition unit	IKI RAS	
HABIT EnvPack		Environmental measurements	Omnysys (Sweden)	Martín-Torres et al. (2020)
Atmospheric temperature sensors ATS	Pt 1000 sensors, 3 per boom (3.6 cm), 3 booms on each of 3 blocks	Measuring atmospheric temperature (±0.2°C), estimating the wind speed and direction (±0.3 m/s)	Omnysys (Sweden)	Gómez-Elvira et al. (2012)
Surface temperature sensor GTS	Remote measurement. Thermocouple (8–14 μm)	Measuring the brightness temperature of the surface (±0.8 °C)	Omnysys (Sweden)	Gómez-Elvira et al. (2012)
UV sensors	Six photodiodes with filters (250–350 nm)	Estimation of UV radiation, ozone content, atmospheric optical density in the UV range	Omnysys (Sweden)	
HABIT BOTTLE	Four containers with salts $CaCl_2$, $Fe_2(SO_4)_3$, $Mg(ClO_4)_2$, $NaClO_4$ and control—mineral dust	Registration of salts transition into liquid state	Omnysys (Sweden)	Martín-Torres et al. (2020)

*Marks additional MTK blocks not related to meteorology.

lated in a hydrostatic approximation. In the lower atmosphere, starting from an altitude of ~5 km and below (after separation of the aerodynamic shield from the lander), the temperature and pressure sensors should operate.

The developments for small stations and penetrators of the Mars-96 project (Harri et al., 1998) served as the basis of MTK. The main sensors (of temperature, pressure, humidity) for the meteorological package were manufactured by the IKI RAS and the Finnish Meteorological Institute (FMI). The paired temperature sensors (one thermistor and a thermocouple) are located on the METEO Boom at heights of 125, 150, and 175 cm from the surface of Mars. To reduce the thermal signature of the boom, the sensors are mounted on 5-cm brackets at different angles. The sensor, measuring the temperature during the descent, was located at a height of 85 cm from the surface after landing (Lipatov et al., 2023b).

The most important pressure sensor is duplicated, a membrane sensor made in-house by IKI RAS and a Barocap® product from Vaisala are used. The Barocap® sensor head is a micro-electromechanical system (MEMS) device made of monocrystalline silicon and is highly stable. Both types of sensors use a change in capacitance between electrodes under the influence of pressure. The sensors were placed in control units (BD and BU of MTK) in different parts of LP. The temperature effect is controlled by thermosensors; corrections are introduced during the data processing.

An ionization anemometer developed and manufactured in IKI RAS was used as a wind speed and direction sensor (Evlanov et al., 2001; Evlanov et al., 2015 [in Russian]). In a rarefied atmosphere, this type of anemometer should provide significantly greater sensitivity compared to commonly used gauges based on the principle of measuring the resistance of heated foil or wire (see, e.g., Gómez-Elvira et al., 2012). An optical dust sensor (ODS) was also developed for small stations. As confirmed by numerous field observations, the course of illumination during the day, measured by photometers with a known field of view at two wavelengths (red and blue channels), makes it possible to accurately estimate the daily average optical depth of the atmosphere and detect clouds (Toledo et al., 2016). Initially developed and validated in France, this sensor was manufactured for MTK by IKI RAS (Khorkin et al., 2023).

Some of the Mars-96 small-station sensors were also planned for installation on small MetNet landing modules developed by Lavochkin Association and IKI RAS, and commissioned by FMI (Harri et al., 2017). Spanish colleagues (Univ. Complutense; INTA, Instituto Nacional de Técnica Aeroespacial) also took part in this project with the SIS sensor, thus defining the circle of main participants in the MTK experiment. The SIS sensor was part of the DREAMS instrument (Esposito et al., 2018) of the *Schiaparelli ExoMars 2016* lander (Arruego et al., 2017; Toledo et al., 2017). The MTK LP included two more Spanish modules,

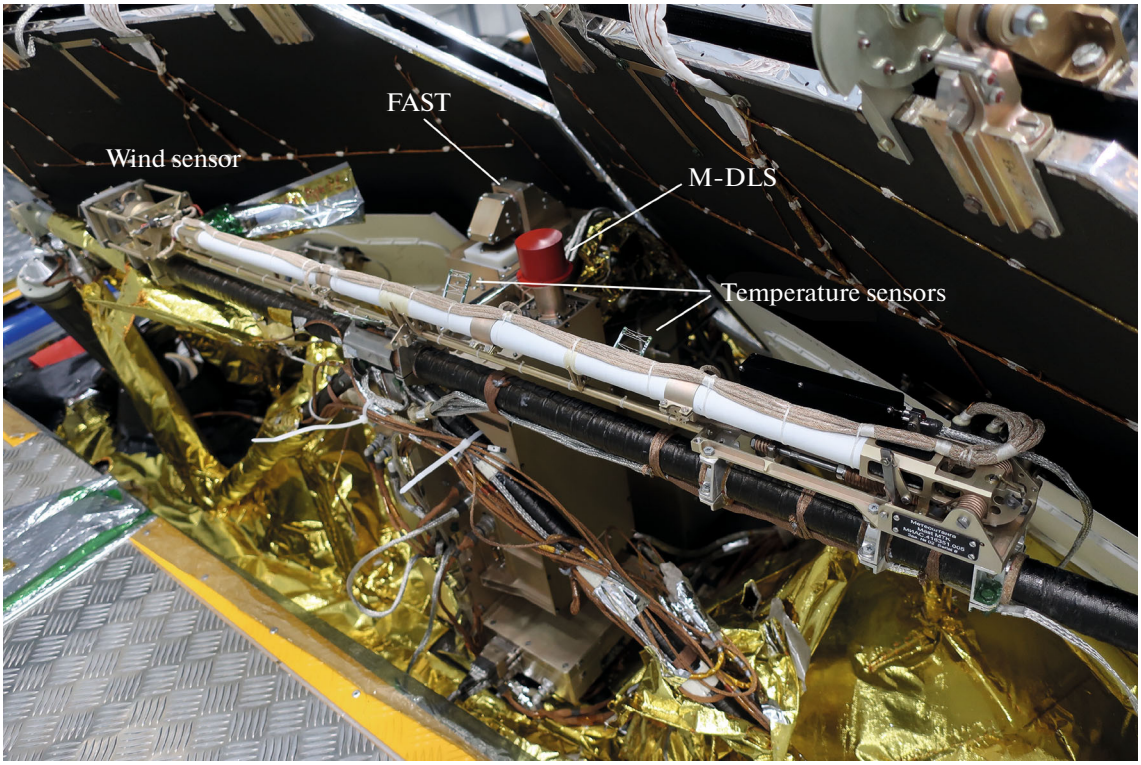

Fig. 3. Folded MTK boom as part of the platform. The base of boom and the deployment mechanism are on the right, the boom top is on the left. Temperature sensors (two out of three are visible) and the wind sensor are shown. The photo also shows the M-DLS air intake closed with a protective cover and the FAST scanner in the parking position (directed at the calibrated blackbody). Photo by IKI RAS.

an infrared nephelometer DS'20 (dust sensor) for determining the local concentration of dust particles, which was developed at Univ. Carlos III and manufactured by INTA, and the AMR magnetometer (see below).

A prototype of the lidar unit was a device developed in the IKI RAS for the unsuccessful NASA Mars Polar Lander project (Arumov et al., 1998). Pointed upward, the lidar was supposed to reconstruct the aerosol profile in the Martian atmosphere to an altitude of ~5 km (Lipatov et al., 2023c), complementing aerosol measurements with passive optical sensors ODS and SIS. Finally, the MTK included a microphone for recording the sounds of Mars and the activity of the LP and rover, which was developed by TsNIIMash and manufactured by IKI RAS.

The SIS block, the wind, temperature and humidity sensors were placed on a meteorological boom—a metal structure 1 m high, which is brought to a vertical position after the rover egress (Fig. 3). SIS was located at the top of the boom (at a height of ~2.2 m above the surface); the wind and humidity sensors were placed below the SIS. Temperature sensors were located at three levels (27, 51 and 75 cm from the base of the boom) on small brackets. The DS'20 block was placed at the base of the METEO Boom. The ODS block was installed on the opposite side of the LP deck.

The main HABIT module, EnvPack, contains a set of temperature sensors (three minibooms 3.6 cm long on each of the three HABIT blocks; three sensors per boom), a ground brightness temperature sensor, and six photodiodes that measure UV radiation. The transmission maxima of the UV filters corresponded to 265, 280, 295, 315 and 330 nm, covering the UV-A, UV-B and UV-C ranges for which the sterilizing ability of UV radiation is standardized. The EnvPack's sensors are based on designs for the *Curiosity* and *Perseverance* rovers (Gómez-Elvira et al., 2012) and its environmental observations would be directly comparable to their data. Thus, to estimate the wind speed and direction, it was supposed to use the technique for processing data from atmospheric temperature sensors, which was developed by Soria-Salinas et al. (2020) for *Curiosity* data.

The BOTTLE unit was intended to track the transition of salts into a liquid state under natural conditions on the surface of Mars (temperature, pressure, humidity) and at elevated temperatures, to assess whether liquid brines could exist on the surface of Mars. Four salts (calcium chloride, ferrous sulfate, magnesium perchlorate and sodium perchlorate) known on Mars, mixed with an absorbent, and a control cell with an analog of Martian dust were used. Dissolution was recorded by means of measuring con-

Table 4. Sensors and subsystems of PK dust suit

Subsystem	Principle of operation	Designation	Main parameters
BUS (IS-1)		Block of impact sensors	Includes PS, QS, OS
Impact sensors (PS)	Piezoelectric sensors (15 pcs)	Measuring the momentum of dust particles	Sensitivity 10 N s
Flyby sensors (QS)	Charge-sensitive flyby sensors (five grids)	Charge and velocity measurements (for charged particles)	Sensitivity 1000 C
Dustiness sensor (OS)	Optical sensor measuring the dust accumulation	Estimation of dustiness on the LP surface	Measurements at three wavelengths: 525, 670, 885 nm
ECS	Measuring the leakage in an open capacitor	Electrical conductivity of atmosphere	10^{11}–10^{13} Ω
MicroMED	Laser nephelometer with pumping	Concentration, particle size distribution	Particles of 0.4–20 μm
PK boom	Extendible boom	Placement of IS-2 closer to surface and ECS away from LP	IS-2 sensors at a height of 10 cm from the surface; EF-1, -2 at a height of 35 and 70 cm from the surface
IS-2	Eight piezo sensors behind a common flyby grid	Measurement of momenta of particles and charge and velocity of charged particles	The same as PS, QS
EF-1, -2	Two electrodes spaced apart in height	Electric field measurement	±1 kV, sensitivity of 60 mV 0–370 Hz
EMA	Antenna	Measuring noise during collisions of charged dust particles	0.12–1.5 MHz

ductivity. The heaters made it possible to use the cells repeatedly. BOTTLE was also positioned as an experiment in obtaining liquid water: testing the possibility of using local resources by manned expeditions.

Dust Suit PK

The dust suit is intended for the contact study of dust particles properties and atmospheric electrical phenomena associated with the transfer of dust (Zakharov et al., 2022). The PK was developed and manufactured by IKI RAS with the participation of the LATMOS laboratory, CNRS (France). The prototype of the main sensors of the instrument was the PmL unit for studying lunar dust (Zakharov et al., 2021). Italian partners (INAF-Osservatorio Astronomico di Capodimonte, Naples) supplied the MicroMED nephelometric unit, a simplified version of a previously developed MEDUSA instrument subsystem (Esposito et al., 2011). The dust suit consisted of the IS-1 main block, two sensors and the PK boom. The PK sensors are located above and below the LP deck, and on the PK boom, closer to the surface. The list of PK sensors is given in Table 4.

The IS-1 block houses piezoelectric (PS) and charge-sensitive (QS) sensors, as well as an optical dustiness sensor (OS). Piezoelectric sensors of the IS-1 block are arranged on five planes of a truncated pyramid. Each plane contains three sensors of different diameters: 4, 15 and 30 mm. The momentum of dust particle is converted into an electrical signal. The sensitivity of the sensors is ~10 N s, which is equivalent, e.g., to the momentum of a 4-μm particle at a speed of ~2 m s^{-1}. The QS sensors are grids placed above each of five piezo-plate planes of IS-1. A charged particle flying by produces a mirror-induced charge, which can be measured. In addition, the delay between the QS signals and the IS-1 piezoelectric sensors determines the velocity and, with a known momentum, the mass of the particle. The IS-2 unit is similarly arranged with two 15- and 30-mm sensors directed in four directions and placed near the surface. At the top of the IS-1 block there is a transparent 20-mm glass, under which there are three LEDs of different colors and photodetectors of the OS sensor. The degree of glass dustiness is determined by the decrease in the intensity of reflected light. The air electric conductivity sensor ECS is a cylindrical capacitor located on the underside of the LP deck near the IS-1 block. The resistance is measured by discharge time.

The PK boom is located near the rover exit ramps placing the IS-2 sensor closer to the surface and the

EF-1, -2 sensors farther away from the LP at a height of 35 and 70 cm from the surface. The electromagnetic activity analyzer (EMA) detects electromagnetic discharges accompanying the motion and collisions of charged dust particles. The 0.9 m long EMA antenna is located within the PK boom. The sensor records an amplitude of the noise signal in the frequency range from 0.12 to 1.5 MHz.

The Italian MicroMED unit is a laser nephelometer, a particle counter in a closed volume with pumping. The volume under study (~0.3 mm^3) is illuminated by a collimated laser beam (0.8 μm) and the light scattered by the particles is recorded by a detector located at an angle of 90°. The intensity and number of signals during a measurement time of 520 s make it possible to determine the number density (~1–100 cm^{-3}) and particle size distribution (0.4–20 μm).

Fourier Spectrometer FAST

The Fourier spectrometer for atmosphere and surface temperature—(FAST)—instrument is designed to study the atmosphere and to monitor the climate of Mars by spectral analysis of solar radiation passing through the planet's atmosphere and the radiation from the atmosphere proper. Also, by observing the thermal radiation of the surface, it is possible to measure its temperature and estimate the mineralogical composition of rocks in the observable vicinity of the LP. The instrument was developed and manufactured at IKI RAS, partly based on technical solutions of the TIRVIM Fourier spectrometer, one of the channels of the ACS spectroscopic complex on the *ExoMars-2016* orbiter (Korablev et al., 2018; Shakun et al., 2018). Unfortunately, there is no generalizing publication on the FAST instrument yet; some information can be found in (Shakun et al., 2017, 2019a, 2019b).

FAST is a monoblock mounted on top on the edge of the LP deck so that its optical input, equipped with a two-axis scanner (Fig. 3), can be oriented to any point in the sky or to the surface. The spectral range of measurements, sensed by an uncooled pyroelectric detector, is 1.7–17 μm. The short-wavelength part of the range (1.7–10 μm) was used in the mode of observing the direct solar radiation, above all, to detect small components of the atmosphere, e.g., methane. The interferometer was assembled according to a scheme with a linear movement of one of the mirrors using a ball-and-screw pair. To detect small components of the atmosphere, the maximum spectral resolution of 0.05 cm^{-1} (without apodization) was chosen, which required an optical path difference of the interferometer of 12.6 cm (when producing a single-sided interferogram); the time of one measurement was 20 min. To carry out these measurements, it was necessary to ensure the simultaneous operation of two optical-mechanical precision systems. One maintained tracking of the solar disk during a long-term observation (Shakun et al., 2019a), another supported the smooth movement of the carriage with the interferometer mirror (Shakun et al., 2019b). In laboratory observations of the Sun at maximum spectral resolution, a relatively low signal-to-noise ratio of ~30, was obtained, however, sufficient for measuring the known small components of the atmosphere (H_2O, CO, O_3) or large methane emissions. Methane detection at a content of 1 ppbv requires a signal-to-noise ratio of ≥500. A cause for the increased noise was, apparently, distortions of the interferogram associated with mechanical disturbances in the operation of the solar tracking system.

For observations of the noise radiation from atmosphere, the spectral resolution was 2 cm^{-1}, the observations were shorter, and no tracking system was used. In this mode, the instrument noise was slightly higher than that of the Mini-TES/Mars Exploration Rovers at a spectral resolution of 10 cm^{-1}. From atmospheric spectra of FAST, it is possible to reconstruct the temperature profile of the surface layers of the atmosphere, by resolving heights from tens of meters to 0.5 km, as well as to measure the optical density of dusty and ice aerosols.

Gas Analysis Package MGAK

The Martian gas analytical package MGAK is designed to study the composition of atmospheric samples using the method of gas chromatography and the following mass spectrometry. The instrument was developed and manufactured at the IKI RAS based on elements of the package (for soil analysis of the pyrolysis method) of the Scientific Equipment Complex for the *Phobos-Grunt* spacecraft. In parallel with *ExoMars*, the development of a similar package for the *Luna-27* project was underway. Unfortunately, there are practically no publications describing any version of the instrument. A conference abstract (Gerasimov et al., 2014) presents the MGAK concept at the proposal stage, when the analysis of both soil and atmospheric samples was planned. The units intended for soil sample preparation and pyrolysis were excluded. Also, the Swiss partners were unable to deliver the time-of-flight mass spectrometer originally planned for *Luna 27* (Hofer et al., 2015). The MGAK of version 2022 consists of two units: a gas chromatograph (GKhM) with two chromatographic columns and a mass spectrometer based on the ion trap principle. The M-DLS laser spectrometer (see below) was separated into an independent instrument, but M-DLS and MGAK have a common system for preparing an atmospheric sample.

Air enters the MGAK through the M-DLS sample preparation system, which includes coarse and fine filters and a number of valves. The suction pump is located in the MGAK package, to which M-DLS is connected by a capillary, i.e., MGAK takes an atmo-

spheric sample through M-DLS. GKhM separates the gas mixture into molecular components, the yield of which is recorded by thermal conductivity detectors. MGAK is a complex system that includes, in addition to the main measuring systems, many auxiliary systems: pumps, a reservoir for gas-carrier (He_2), heated capillaries, microvalve blocks, etc. Two capillary columns with molecular sieves 5A and PoraPlot Q, separating the permanent and noble gases, were used. Before the analysis, gases can pass through enrichment traps, which increase the concentration of trace gas components due to their accumulation on adsorbents and the subsequent extraction for analysis. Each column had its own injection trap. After each measurement, the entire system was heated up. The duration of a typical MGAK measurement cycle was about 1 h.

The mass spectrometer for neutral gases was manufactured at IKI RAS based on a similar device as part of the Ptolemy/Rosetta instrument (Todd et al., 2007). This type of mass spectrometer is compact and allows operation in a low vacuum. It operates in the mass/charge range of 12–50 (from water to xenon) and measures isotope ratios. The mass spectrometer was evacuated with a dedicated pump to $\leq 10^{-4}$ Torr.

Laser Spectrometer M-DLS

The M-DLS multichannel diode laser spectrometer is designed to study the composition of atmospheric samples using the spectroscopy of ultrahigh resolution. The instrument was developed and manufactured at IKI RAS in close collaboration with MIPT (Rodin et al., 2020). The prototype of the instrument is a similar device that was part of the gas analytical unit of the Scientific Equipment Complex on the *Phobos-Grunt* spacecraft (Durry et al., 2010).

M-DLS is a monoblock with a head for taking atmospheric samples (Fig. 3), which is connected by a capillary to the gas chromatograph GKhM unit of MGAK package. The device analyzes an atmospheric sample in a multipass optical cell, recording the absorption in individual spectral lines of atmospheric gases in the near-IR range. The lines are detected by tuning the wavelength of a semiconductor laser diode. The range of this tuning (by modulating the laser pump current) is usually no more than 1 cm^{-1}, and, as a rule, each gas requires its own laser. The spectral resolution is ~0.002 cm^{-1}. The instrument implements the principle of integrated resonator spectroscopy. The main element—the integrated cavity optical spectroscopy (ICOS) cell—is a pair of spherical mirrors separated by a distance (22 cm), slightly less than their focus. Off-axis beam injection into the cell produces many transverse modes, filling densely the resonator, and provides (depending on the reflection coefficients of the mirrors) the effective optical path from the laser to the detector up to 110 m. Two lasers (2.656 and 2.808 μm) were used to record the absorption lines of CO_2, H_2O and their isotopologues. The range includes seven lines of the main isotopologue of CO_2 and one of each of $^{16}O^{12}C^{18}O$, $^{16}O^{12}C^{17}O$, $^{13}C^{16}O_2$, as well as three lines of the main isotopologue of H_2O and a single line of each of $HD^{16}O$, $H_2{}^{18}O$.

Before measurement, the cell was evacuated; to increase sensitivity the pressure can be increased from an atmospheric value (5–10 mbar) to ~30 mbar. One measurement took 6 min; with accumulation, the measurement duration reached 90 min. In laboratory tests, the accuracy of measuring the isotope ratios was demonstrated to be close to the accuracy of spectroscopic line parameters in the HITRAN database.

Radiometer RAT-M

The microwave radiometer RAT-M (RAdioThermometer for Mars or PlAnk Thermometer for Mars) is designed to measure surface brightness temperature in three ranges (6, 8 and 15 GHz). The device was developed and manufactured at IKI RAS under the direction of D.P. Skulachev; there are no publications on the device.

RAT-M is a monoblock with two horn antennas, one of which is aimed at the surface, and the other at the zenith. The antenna radiation pattern is wide: ~45°. The emission from the surface in the ~1 GHz band is compared with the signal from the atmosphere, which is almost transparent in the microwave range with a low dust content. The expected thickness of the skin layer of the Martian regolith for wavelengths from 1.7 to 3 cm will be from 5 to 50 cm, making it possible to estimate the ground temperature profile down to a depth of 1 m and record its daily and seasonal changes. The sensitivity of the device is ~0.25 K.

RAT-M also provides an opportunity to estimate an optical depth of the atmosphere under conditions of global or regional dust storms. The reference signal in this case becomes the main one. The attenuation of microwave radiation by dust particles in the atmosphere is determined by Rayleigh scattering, and the brightness temperature of the sky during a dust storm (5–50 K) is a measurable quantity, even accounting for ground temperature uncertainties. Thus, RAT-M could estimate the dust content in the atmosphere when the optical depth becomes too large to be measured in the visible (MTK sensors) or IR (FAST) ranges.

Active Neutron and Gamma Spectrometer with Dosimetry Unit ADRON-EM

ADRON-EM combines five functional units: a pulse neutron generator (PNG), detectors of neutrons (DN), a gamma-radiation detector (GD), a dosimeter module (DM) and a module of electronics (ME). The DN, GD and ME modules are combined into a com-

mon block of detectors and electronics; the PNG and dosimeter are separate blocks. ADRON-EM was developed and manufactured at IKI RAS based on previously developed DAN/Curiosity (Mitrofanov et al., 2012) and MGNS/Bepi Colombo (Mitrofanov et al., 2021), and in parallel with the development of ADRON-RM for the Rosalind Franklin rover (Mitrofanov et al., 2017) and ADRON-LR (Golovin et al., 2021) instruments. The PNG unit, a generator of neutron pulses for irradiating surface matter, was developed and manufactured at the N.L. Dukhov VNIIA. Such a device was first used in space within the DAN/Curiosity instrument.

The surface hydration was assessed by measuring a flux of neutrons produced at a depth of 1–2 m as a result of interaction of the high-energy charged particles from galactic cosmic rays (GCRs) or the neutrons activated by a neutron-pulse generator PNG. The nuclei of light elements, especially hydrogen, effectively slow down the fast neutrons due to their similar masses.

Detectors of neutrons (DN module of two proportional ^{3}He counters) record neutrons with energies from 0.05 eV to 1 keV. One of the counters is surrounded by a cadmium shield which is opaque to thermal neutrons (≤0.4 eV). Thus, the difference in the detector count rate corresponds to the contribution of thermal neutrons.

The PNG unit generates neutron pulses with an energy of 14.4 MeV when accelerated deuterium ions collide with a tritium target. The pulse duration is ~2 μs, the repetition rate is up to 10 Hz. Pulses with a duration of ~2 μs penetrate into the soil of Mars to a depth of about 1 m. Inelastic scattering reactions occur within tens of microseconds after the neutron pulse, and the recording of the delay of secondary neutron emission makes it possible to reconstruct the soil hydration profile to a depth of ~0.5 m in 0.1 m increments.

The gamma spectrometer (GD unit) registers gamma rays in the range from 200 keV to 7 MeV. A scintillation detector based on $CeBr_3$ with a spectral resolution better than 4.5% at 662 keV was used. Neutrons interact with the nuclei of matter in reactions of inelastic scattering and capture, which are accompanied by the emission of gamma rays. In addition, irradiation produces short-lived isotopes, whose decay is also accompanied by gamma radiation. Measuring the gamma spectrum provides information about the content of the main rock-forming elements (O, Si, Al, Fe, Mg, Na, Ca) and radiogenic elements (K, U, Th) in minerals in the immediate (≤3 m) vicinity of the landing site. In parallel, the density of the soil is measured.

The ADRON-DM (Lulin-ML) module is designed for monitoring the radiation situation (determination of the radiation dose from charged particles). The module was developed and built at the Institute of Space Research and Technology of the Bulgarian Academy of Sciences, Sofia, based on the Lulin line of instruments (see, e.g., Semkova et al., 1994; Mitrofanov et al., 2018). The device contains two perpendicular dosimetric telescopes, each of which consists of two silicon PIN photodiodes with a thickness of 0.3 mm and an area of 2 cm^2, spaced at a distance of 21 mm. The device measured the absorbed dose rate in the range of 10^{-6}–1 Gy/h and the energy transfer spectrum from 60 keV to 180 MeV. The spectra accumulation time was 1 h.

MAIGRET and AMR Magnetometers

The MAIGRET equipment (Martian ground electromagnetic tool) consists of three blocks, the LEMI SEM boom and the UF-M sensor and an electronics unit. Functionally, it includes the search-coil and fluxgate magnetometers, an electric field antenna and a spectrum analyzer. The device was developed in IKI RAS under the leadership of A.V. Skalsky with a key contribution from the Institute of Atmospheric Physics (Czech Republic), which supplied a search-coil magnetometer and a wave analyzer module (WAM) that is part of the MAIGRET electronics unit (Kolmasova et al., 2017). Unfortunately, there are no other publications on the device. The predecessor of MAIGRET was a complex for plasma-wave measurements (FPMS) on the *Phobos-Grunt* spacecraft. Figure 4 shows the LEMI SEM block at the LP.

MAIGRET measures quasi-constant (±30 000 nT, frequencies up to 32 Hz) magnetic and alternating (0.1–40 kHz) electromagnetic fields. It is designed to record crustal magnetization and its variations, electromagnetic radiation coming from space, and atmospheric electrical discharges occurring during dust events.

The anisotropic magnetoresistance (AMR) magnetometer (Díaz Michelena et al., 2023) is a two-vector magnetoresistive sensor with a deployment device that ejects it 2 m from the LP. The device was developed and built at INTA (Instituto Nacional de Técnica Aeroespacial) in Spain. The measurement range is ±150 μT with a resolution of 1 nT and noise of ~0.5 nT $Hz^{-½}$. The device was part of the MTK package and was controlled by the MTK-L unit, which supported the AMR operation both during a descent (from an altitude of ~125 km) and on the surface. This would test the accuracy of models that extrapolate measurements of the magnetic field of Mars from the orbit to the surface. Also, due to deployment away from the non-magnetically pure platform, AMR would make it possible to refine MAIGRET's quasi-permanent magnetic field measurements.

Seismometer SEM

The seismometer for *ExoMars* (SEM) is designed to measure microvibrations of the Martian surface, its

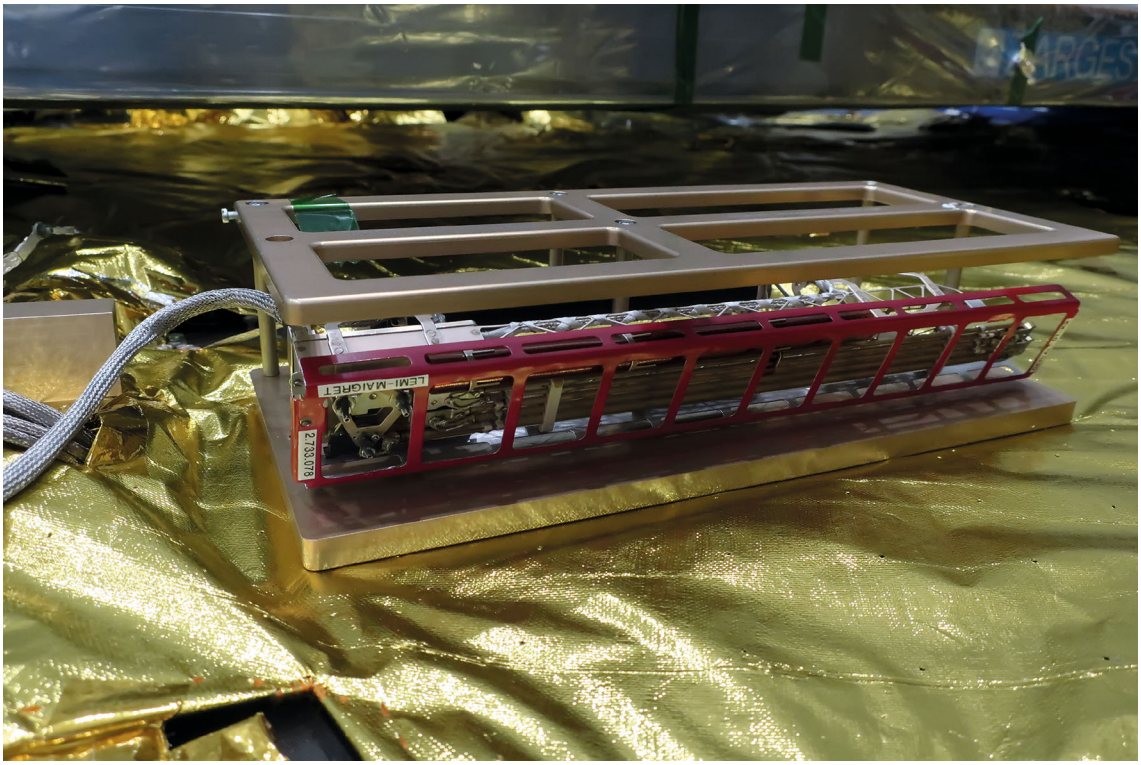

Fig. 4. LEMI SEM block. Photo by IKI RAS.

quasi-static motions and variations in the gravitational field (Manukin et al., 2021). This is a new development of IKI RAS with the participation of the Schmidt Institute of the Physics of the Earth of Russian Academy of Sciences. The GRAS-F microgravimeter of the Phobos-Grunt project can be considered a distant prototype of the device (Manukin et al., 2010). The instrument is a monoblock, the main volume of which is determined by the deployment system. It should ensure a contact of the sensors with the surface and their isolation from vibrations of the LP and wind.

The sensor part consists of three identical uniaxial accelerometers installed at an angle of 90° symmetrically relative to the gravitational vertical. In each channel, a cylindrical test mass (50 g) was suspended on six elastic beryllium-bronze elements, so that it could move only along one coordinate. The linear movement was recorded from changes in capacitance. The SEM measures slow slopes over a range of $\pm 3 \times 10^{-3}$ deg with a sensitivity of 3×10^{-9} for periods from 100 s to months and gravitational acceleration variations up to 1.7×10^{-2} m s^{-2} with a sensitivity of ~10^{-9} m s^{-2}. Surface vibrations along three axes are measured in the frequency range 0.1–10 Hz with an amplitude sensitivity of ~4×10^{-11} m per 1 Hz.

The deployment system was to install the SEM under the LP body. The protective casing with the device was lowered to the surface using a pantograph (Fig. 5), and then the device freely fell from a height of 5–10 mm. To verticalize, an orientation system suspended the sensor unit on a gimbal along the local gravitational vertical using an electromagnet; then, after removing the voltage from the electromagnet, the system lowered it onto the support. If necessary, this operation could be repeated many times. To ensure the device operation in continuous monitoring mode, the device was qualified in the temperature range from –130°C to +60°C.

Coherent LaRa Transponder

The Lander Radioscience (LaRa) device is designed for high-precision determination of parameters of the proper motion and rotation of Mars. The Doppler shift of the radio signal between the LP on the surface of Mars and the ground stations is used (Dehant et al., 2020). The device was developed in Belgium under the direction of the Royal Observatory of Belgium and manufactured by the Belgian company OHB Antwerp Space. The device consists of a transponder and three disk antennas: two transmitting and one receiving. The experiment to measure the relative position of Mars and Earth includes a ground segment, for which the NASA DSN and ESA ESTRACK antennas were planned to be used. The use of the Russian station in Kalyazin was also considered.

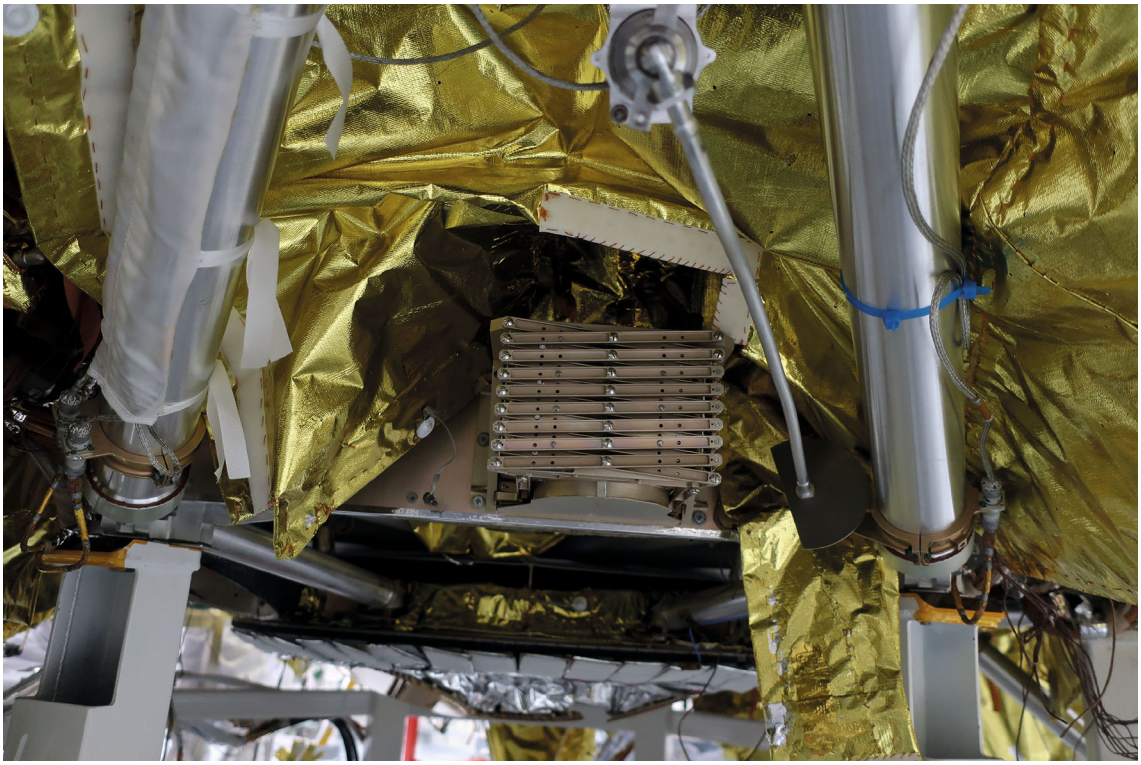

Fig. 5. Lower part of LP. The pantograph of the SEM deployment system can be seen. Photo by IKI RAS.

LaRa is an X-band transceiver that preserves the phase of the received signal. A highly stable signal with a frequency of 7.2 GHz was sent from Earth, and a frequency of 8.4 GHz was transmitted back. Transmitter output power is 5 W with a consumption of 42 W.

Interface and Memory Block, BIP

BIP is designed to control the SIC instruments, as well as to receive, store and transmit scientific information from the instruments. On the one side, the instruments are connected to BIP; on the other side, an onboard computer (OBC) of the LP is connected. BIP is connected to the OBC via the MIL 1553 interface. BIP is responsible for issuing digital commands to devices in accordance with the cyclogram, for acquiring data of all devices, handling emergency situations during the SIC operation, storing data in nonvolatile memory and transmitting data to the LP radio channel (via OBC). Power supply to the devices was supplied directly from the LP. BIP was created at the IKI RAS on the basis of numerous developments for other projects. A brief description and diagram of a similar electronics unit of the ACS/ExoMars-2016 instrument can be found in (Korablev et al., 2018).

SCIENCE OPERATIONS PLAN

The main factor limiting the SIC operation on the surface was the amount of data available for transmission to Earth. It should be implemented through orbiters around Mars (nominally, through the TGO spacecraft). The same communication channel is used by the rover. For the LP, an average available volume of 150 Mbit per sol (Martian day) was agreed under condition of equal channel sharing between the LP and the rover. In reality, some flexibility was allowed for dividing this volume to maximize the scientific return on the project. In addition, BIP could store a significant amount of information allowing data accumulation and their transmission to Earth when the opportunity arises.

The power consumption of all SIC devices at the entry descent and landing (EDL) stage should not exceed 30 W. During the work on the surface, power consumption should not exceed 120 W during the day and 25 W at night. The length of the day is assumed to be 10 local hours.

The main stages of the project are divided into the phase of flight to Mars (Cruise), descent into the atmosphere and landing (EDL phase), the phase after landing and before the rover's departure, and the phase of routine operations on the surface.

At the Cruise stage, it was planned to carry out the test switching-on of instruments, with the exception of the antennas of the LaRa device, and the operation of the ADRON-EM device in passive mode, including the dosimetric module for the maximum possible time.

EDL Phase (Entry, Descent and Landing)

The landing module enters the atmosphere at a velocity of ~5.5 km/s. From an altitude of ~120 km, it starts decelerating due to the atmospheric drag for ~3 min. At an altitude of 8–10 km, the first (supersonic) parachute with a diameter of 16 m (velocity of 2 M, 470 m/s) opens. After 20 s, at an altitude of 4–6 km, the second (subsonic) parachute with a diameter of 35 m opens (velocity of 0.6 M, ~150 m/s). After 10 s, at an altitude of 3–5 km (velocity of 64 m/s), the aerodynamic shield is jettisoned, the legs of the LP are extended, and the spin is compensated for. From an altitude of 2 km, the radio altimeter begins to track the altitude and velocity vector. According to these data, at an altitude of ~1 km above the surface (velocity of 36 m/s), the rear shroud and parachute separate and the LP goes into a free fall for about 1 s. This is done to increase vertical separation from the rear shroud and parachute. The lander then performs a lateral collision avoidance maneuver (10 s) and proceeds to intensive braking for 7 s—the last 500 m—until touchdown at a speed of ≤2 m/s.

During the EDL, a part of the meteorological package (MTK-L, including the AMR magnetometer) and the TSPP-EM cameras were supposed to operate. Both instruments had their own control electronics with nonvolatile memory, which ensured their autonomous operation without the BIP involvement. The switching of the BIP was not provided in order to completely eliminate its influence on the OBC during the critical descent phase.

MTK-L is turned on within 3 min after the separation of the lander from the cruise module and operates autonomously until landing. Power consumption is ~2 W. Before the aerodynamic shield separates, the accelerometer and AMR (until landing) are interrogated, then the pressure and temperature sensors are queried (until landing). After the parachute system separates, the lidar is turned on (until landing).

TSPP-EM is activated 200 s before landing, and since that moment with all four cameras it shoots video in 512×512 format, 10 frames per second. The 11-Gbit video can be reduced by selecting the frame rate and transmitted to Earth when it is possible to transmit a significant amount of data without affecting

	00	01	02	03	04	05	06	07	08	09	10	11	12	13	14	15	16	17	18	19	20	21	22	23
BIP									+	+	+	+	+	+	+	+	+	+						
PK	+	+	+	+	+	+	+	+	+	+	+	+	+	+	+	+	+	+	+	+	+	+	+	+
MTK	+	+	+	+	+	+	+	+	+	+	+	+	+	+	+	+	+	+	+	+	+	+	+	+
MAIGRET									+	+	+	+	+	+	+	+	+	+						
SEM	+	+	+	+	+	+	+	+	+	+	+	+	+	+	+	+	+	+	+	+	+	+	+	+
RAT-M										+		+		+		+		+						
Habit	+	+	+	+	+	+	+	+	+	+	+	+	+	+	+	+	+	+	+	+	+	+	+	+
ADRON-EM Pass/Dos									+	+	+	+	+	+	+	+	+	+						

	00	01	02	03	04	05	06	07	08	09	10	11	12	13	14	15	16	17	18	19	20	21	22	23
BIP									+	+	+	+	+	+	+	+	+	+						
PK	+	+	+	+	+	+	+	+	+	+	+	+	+	+	+	+	+	+	+	+	+	+	+	+
MTK	+	+	+	+	+	+	+	+	+	+	+	+	+	+	+	+	+	+	+	+	+	+	+	+
MAIGRET									+	+	+	+	+	+	+	+	+	+						
SEM	+	+	+	+	+	+	+	+	+	+	+	+	+	+	+	+	+	+	+	+	+	+	+	+
RAT-M										+		+		+		+		+						
Habit	+	+	+	+	+	+	+	+	+	+	+	+	+	+	+	+	+	+	+	+	+	+	+	+
ADRON-EM Pass/Dos									+	+	+	+	+	+	+	+	+	+						

Fig. 6. Examples of SIC operation scenarios on the surface. (a) Monitoring sol 1: at night, MTK, HABIT, PK, and SEM work, BIP is turned off; in the daytime, all monitoring devices operate, data volume is ~6.3 MB, maximum power consumption is 25 W (night), 49 W (day). (b) Operating scenario for MGAK and M-DLS devices: any monitoring sol and daytime operation of MGAK and M-DLS devices. Monitoring sol 3 is given as an example: data volume ~13.0 MB, maximum power consumption is 21 W (night), 84 W (day).

other scientific instruments. After landing, BIP is turned on and, at its command, a panorama of maximum definition is shot. A full panorama takes 90 Mbit.

After landing and before the rover moves away, also with the help of TSPP-EM cameras and by commands from BIP, the rover's egress and moving is supported. A priority during this time was given to operations related to the rover. To extend the range of weather observations, provision was made for switching on MTK-L (pressure and temperature sensors) in the offline mode.

Phase of Surface Operations

After the rover leaves, the landing platform begins its nominal scientific activities. The necessary preparatory procedures are carried out: unfolding the MTK and PK booms, installing the SEM sensor on the surface, deploying the M-DLS sampling system, the AMR magnetometer, calibrating the SIC instruments.

The SIC devices can be divided into two groups: the devices requiring a permanent operation in the monitoring mode (MTK, MAIGRET, RAT-M, HABIT, PK, SEM, ADRON-EM in the passive mode with a dosimeter), and those not requiring permanent operation (FAST, MGAK, M-DLS, TSPP-EM, LaRa, ADRON-EM in the active mode). At night, the operation of monitoring devices is limited to a total power consumption of ≤25 W. The priority was given to devices that can operate without BIP, accumulating data for transmission to BIP during the day. All monitoring devices except ADRON-EM had this capability.

For planning purposes, a number of standard sequences per sol were developed. They can be divided into three main categories: monitoring sols (the main difference is the night operation); monitoring sols and daytime operation of other devices, and energy-saving scenarios, e.g., in case of emergency situations or when the LP batteries need to be recharged. To obtain the desired cyclogram, various scenarios could be combined. In addition, it was planned to develop scenarios on requests that would be executed once during the entire period of work on the surface. Examples of scenarios are shown in Fig. 6.

CONCLUSIONS

In the ExoMars project, remote sensing of Mars from an orbiter around Mars—the *Trace Gas Orbiter* (ExoMars-2016)—was supposed to be complemented by the complex of scientific instrumentation of the landing platform and the *ExoMars-2022* rover on the surface. A wide range of studies was planned, including the monitoring of climate, exploration of atmospheric composition, mechanisms of dust lifting, interactions between the atmosphere and the surface, subsurface water abundance, monitoring of radiation and the studies of internal structure.

Many objectives were of a high priority, relevant experiments were planned for the first time or would compete with single analogs. These include studies of the mechanisms of dust lifting and the occurrence of dust storms, two-point seismometry with *InSight*, measurements of the magnetic field profile during a descent, comprehensive studies of atmosphere–surface interaction, etc. Simultaneous measurements with *InSight* could not take place: the project was postponed twice for objective reasons (development delay in 2018 and pandemic in 2020). Also, two instruments, initially aiming at top-priority measurements of biogenic gases (methane) from the surface, lost their corresponding functionality during the development process for various reasons. The capabilities of the remaining experiments were fully confirmed during the testing and calibration of flight units of SIC instruments.

After the termination of work on the project, a fully completed and tested space complex remained. We hope to continue research and pursue some of the planned experiments, probably in cooperation with new partners.

FUNDING

This work was supported by ongoing institutional funding. No additional grants to carry out or direct this particular research were obtained.

CONFLICT OF INTEREST

The authors of this work declare that they have no conflicts of interest.

REFERENCES

Aboudan, A., Colombatti, G., Bettanini, C., Ferri, F., Lewis, S., Van Hove, B., Karatekin, O., and Debei, S., *ExoMars 2016* Schiaparelli Module trajectory and atmospheric profiles reconstruction. Analysis of the onboard inertial and radar measurements, *Space Sci. Rev.,*

2018, vol. 214, p. 97.
https://doi.org/10.1007/s11214-018-0532-3

Abramov, N.F., Polyanskii, I.V., Prokhorova, S.A., and El'yashev, Ya.D., Ground testing of the landing platform television system of the ExoMars-2022 spacecraft, *Sol. Syst. Res.,* 2023, vol. 57, no. 5, pp. 405–413.
https://doi.org/10.1134/S0038094623040019

Acuna, M.H., Connerney, J.E.P., Ness, N.F., Lin, R.P., Mitchell, D., Carlson, C.W., McFadden, J., Anderson, K.A., Rème, H., Mazelle, C., Vignes, D., Wasilewski, P., and Cloutier, P., Global distribution of crustal magnetization discovered by the *Mars Global Surveyor* MAG/ER experiment, *Science,* 1999, vol. 284, p. 790.
https://doi.org/10.1126/science.284.5415.790

Alday, J., Trokhimovskiy, A., Irwin, P.G.J., Wilson, C.F., Montmessin, F., Lefevre, F., Fedorova, A.A., Belyaev, D.A., Olsen, K.S., Korablev, O., and 6 co-authors, Isotopic fractionation of water and its photolytic products in the atmosphere of Mars, *Nat. Astron.,* 2021a, vol. 5, pp. 943–950.
https://doi.org/10.1038/s41550-021-01389-x

Alday, J., Wilson, C.F., Irwin, P.G.J., Trokhimovskiy, A., Montmessin, F., Fedorova, A.A., Belyaev, D.A., Olsen, K.S., Korablev, O., Lefévre, F., and 4 co-authors, Isotopic composition of CO_2 in the atmosphere of Mars: Fractionation by diffusive separation observed by the *ExoMars* Trace Gas Orbiter, *J. Geophys. Res.: Planets,* 2021b, vol. 126, p. e06992.
https://doi.org/10.1029/2021JE006992

Anderson, D.L., Miller, W.F., Duennebier, F.K., Toksoz, M.F., Kovach, R.L., Knight, T.C.D., Lazarewicz, A.R., Miller, W.F., Nakamura, Y., and Sutto, G., The *Viking* seismic experiment, *Science,* 1976, vol. 194, no. 4721, pp. 1318–1321.
https://doi.org/10.1126/science.194.4271.1318

Arruego, I., Apéstigue, V., Jimenez-Martin, J., Martinez-Oter, J., Alvarez-Rios, F.J., Gonzalez-Guerrero, M., Rivas, J., Azcue, J., Martin, I., Toledo, D., and 3 co-authors, DREAMS-SIS: The Solar Irradiance Sensor on-board the *ExoMars 2016* lander, *Adv. Space Res.*, 2017, vol. 60, pp. 103–120.
https://doi.org/10.1016/j.asr.2017.04.002

Arumov, G.P., Bukharin, A.V., Linkin, V.M., Lipatov, A.N., Lyash, A.N., Makarov, V.S., Pershin, S.M., and Tiurin, A.V., Compact aerosol lidar for Martian atmosphere monitoring according to the NASA Mars Surveyor Program, *'98 Proc. SPIE,* 1999, vol. 3688, p. 494.
https://doi.org/10.1117/12.337558

Atreya, S.K., Wong, A.-S., Renno, N.O., Farrell, W.M., Delory, G.T., Sentman, D.D., Cummer, S.A., Marshall, J.R., Rafkin, S.C.R., and Catling, D.C., Oxidant enhancement in Martian dust devils and storms: implications for life and habitability, *Astrobiology,* 2006, vol. 6, pp. 439–450.
https://doi.org/10.1089/ast.2006.6.439

Atreya, S.K., Trainer, M.G., Franz, H.B., Wong, M.H., Manning, H.L.K., Malespin, C.A., Mahaffy, P.R., Conrad, P.G., Brunner, A.E., Leshin, L.A., and 5 co-authors, Primordial argon isotope fractionation in the atmosphere of Mars measured by the SAM instrument on *Curiosity* and implications for atmospheric loss, *Geophys Res. Lett.,* 2013, vol. 40, pp. 5605–5609.
https://doi.org/10.1002/2013GL057763

Avduevskii, V.S., Akim, E.L., Aleshin, V.I., Borodin, N.F., Kerzhanovich, V.V., Mal'kov, Ya.V., Marov, M.Ya., Morozov, S.F., Rozhdestvenskii, M.K., Ryabov, O.L., Subbotin, M.I., Suslov, V.M., Cheremukhina, Z.P., and Shkirina, V.I., The atmosphere of Mars in the landing area of the *Mars-6* lander (preliminary results), *Kosm. Issled.,* 1975, vol. 13, pp. 21–32.

Blanchard, R.C. and Desai, P.N., *Mars Phoenix* entry, descent, and landing trajectory and atmosphere reconstruction, *J. Spacecr. Rockets,* 2011, vol. 48, pp. 809–821.
https://doi.org/10.2514/1.46274

Chamberlain, T.E., Cole, H.L., Dutton, R.G., Greene, G.C., and Tillman, J.E., Atmospheric measurements on Mars: The *Viking* meteorology experiment, *Am. Meteorol. Soc. Bull.,* 1976, vol. 57, p. 1094.
https://doi.org/10.1175/1520-0477(1976)057<1094:AMOMTV>2.0.CO;2

Ciarletti, V., Clifford, S., Plettemeier, D., Le Gall, A., Herve, Y., Dorizon, S., Quantin-Nataf, C., Benedix, W.-S., Schwenzer, S., Pettinelli, E., and 7 co-authors, The WISDOM radar: Unveiling the subsurface beneath the *ExoMars* rover and identifying the best locations for drilling, *Astrobiology,* 2017, vol. 17, pp. 565–584.
https://doi.org/10.1089/ast.2016.1532

Connerney, J.E.P., Espley, J.R., DiBraccio, G.A., Gruesbeck, J.R., Oliversen, R.J., Mitchell, D.L., Halekas, J., Mazelle, C., Brain, D., and Jakosky, B.M., First results of the MAVEN magnetic field investigation, *Geophys. Rev. Lett.,* 2015, vol. 42, pp. 8819–8827.
https://doi.org/10.1002/2015GL065366

Conrad, P.G., Malespin, C.A., Franz, H.B., Pepin, R.O., Trainer, M.G., Schwenzer, S.P., Atreya, S.K., Freissinet, C., Jones, J.H., Manning, H., and 5 co-authors, In situ measurement of atmospheric krypton and xenon on Mars with Mars Science Laboratory, *Earth Planet. Sci. Lett.,* 2016, vol. 454, pp. 1–9.
https://doi.org/10.1016/j.epsl.2016.08.028

Daerden, F., Whiteway, JA., Neary, L., Komguem, L., Lemmon, M.T., Heavens, N.G., Cantor, B.A., Hebrard, E., and Smith, M.D., A solar escalator on Mars: Self-lifting of dust layers by radiative heating, *Geophys. Res. Lett.,* 2015, vol. 42, pp. 7319–7326.
https://doi.org/10.1002/2015GL064892

Dehant, V., Le Maistre, S., Baland, R.-M., Bergeot, N., Karatekin, O., Peters, M.-J., Rivoldini, A., Lozano, L.R., Temel, O., Van Hoolst, T., and 11 co-authors, The radioscience LaRa instrument onboard *ExoMars 2020* to investigate the rotation and interior of Mars, *Planet. Space Sci.,* 2020, vol. 180, p. 104776.
https://doi.org/10.1016/j.pss.2019.104776

Díaz Michelena, M., Rivero, M.Á., Romero, S.F., Adeli, S., Oliveira, J.S., Henrich, C., Aspás, A., and Parrondo, M., Anisotropic MagnetoResistance (AMR) instrument to study the Martian magnetic environment from the surface: Expected scientific return, *Sol. Syst. Res.,* 2023, vol. 57, pp. 307–323.
https://doi.org/10.1134/S003809462304010X

Durry, G., Li, J.S., Vinogradov, I., Titov, A., Joly, L., Cousin, J., Decarpenterie, T., Amarouche, N., Liu, X., Parvitte, B., Korablev, O., Gerasimov, M., and Zéninari, V., Near infrared diode laser spectroscopy of

C_2H_2, H_2O, CO_2 and their isotopologues and the application to TDLAS, a tunable diode laser spectrometer for the Martian *Phobos-Grunt* space mission, *Appl. Phys. B,* 2010, vol. 99, pp. 339–351. https://doi.org/10.1007/s00340-010-3924-y

Ehresmann, B., Zeitlin, C., Hassler, D.M., Guo, J., Wimmer-Schweingruber, R.F., Berger, T., Matthiä, D., and Reitz, G., The Martian surface radiation environment at solar minimum measured with MSL/RAD, *Icarus*, 2023, vol. 393, p. 115035. https://doi.org/10.1016/j.Icarus.2022.115035

Esposito, F., Colangeli, L., Della, CorteV., Molfese, C., Palumbo, P., Ventura, S., Merrison, J., Nornberg, P., Rodriguez-Gomez, J.F., Lopez-Moreno, J.J., and 7 co-authors, MEDUSA: Observation of atmospheric dust and water vapor close to the surface of Mars, *Int. J. Mars Sci. Expl.,* 2011, vol. 6, pp. 1–12.

Esposito, F., Debei, S., Bettanini, C., Molfese, C., Arruego Rodríguez I., Colombatti G., Harri A.-M., Montmessin F., Wilson C., Aboudan A., and 58 co-authors, The DREAMS experiment onboard the Schiaparelli module of the *ExoMars 2016* mission: Design, performances and expected results, *Space Sci. Rev.,* 2018, vol. 214, p. 103. https://doi.org/10.1007/s11214-018-0535-0

Evlanov, E.N., Zav'yalov, M.A., Podkolzin, S.N., Rodionov, D.S., Tyuryukanov, P.M., Lipatov, A.N., and Ekonomov, A.P., Gas discharge anemometer, *Datchiki i sistemy,* 2015, vol. 190, no. 3, pp. 47–50.

Evlanov, E.N., Zubkov, B.V., Nenarokov, D.F., Linkin, V.M., Zavjalov, M.A., and Tyuryukanov, P.M., Gas-discharge anemometer for the investigation of flow dynamics in rarefied gas media, *Cosmic Res.,* 2001, vol. 39, no. 5, pp. 453–458.

Ferri, F., Karatekin, Ö., Lewis, S.R., Forget, F., Aboudan, A., Colombatti, G., Bettanini, C., Debei, S., Van Hove, B., Dehant, V., and 18 co-authors, ExoMars Atmospheric Mars Entry and Landing Investigations and Analysis (AMELIA), *Space Sci. Rev.*, 2019, vol. 215, p. 8. https://doi.org/10.1007/s11214-019-0578-x

Folkner, W.M., Yoder, C.F., Yuan, D.N., Standish, E.M., and Preston, R.A., Interior structure and seasonal mass redistribution of Mars from radio tracking of Mars Pathfinder, *Science,* 1997, vol. 278, pp. 1749–1752. https://doi.org/10.1126/science.278.5344.1749

Forget, F., Hourdin, F., Fournier, R., Hourdin, C., Talagrand, O., Collins, M., Lewis, S.R., Read, P.L., and Huot, J.-P., Improved general circulation models of the Martian atmosphere from the surface to above 80 km, *J. Geophys. Res.: Planets,* 1999, vol. 104, pp. 24155–24175. https://doi.org/10.1029/1999JE001025

Franz, H.B., Mahaffy, P.R., Webster, C.R., Flesch, G.J., Raaen, E., Freissinet, C., Atreya, S.K., House, C.H., McAdam, A.C., Knudson, C.A., and 12 co-authors, Indigenous and exogenous organics and surface-atmosphere cycling inferred from carbon and oxygen isotopes at gale crater, *Nat. Astron.,* 2020, vol. 4, pp. 526–532. https://doi.org/10.1038/s41550-019-0990-x

Gerasimov, M.V., Sapgir, AG., Zaitsev, M.A., Aseev, S.A., Vinogradov, I.I., Szopa, C., Coll, P., Cabane, M., Coscia, D., Goesmann, F., Wurz, P., Lasi, D., and Tulej, M., *The Martian gas-analytic package for the landing platform experiments of the ExoMars 2018*, *Proc. LPI,* 2014, p. 1242. https://www.hou.usra.edu/meetings/lpsc2014/pdf/1242.pdf.

Giardini, D., Lognonne, P., Banerdt, W.B., Pike, W.T., Christensen, U., Ceylan, S., Clinton, J.F., van Driel, M., Stahler, S.C., Bose, M., and 53 co-authors, The seismicity of Mars, *Nat. Geosci.,* 2020, vol. 13, pp. 205–212.

Golovin, D.V., Mokrousov, M.I., Mitrofanov, I.G., Kozyrev, A.S., Litvak, M.L., Malakhov, A.V., Nikiforov, S.Yu., Sanin, A.B., Barmakov, Y.N., Bogolubov, E.P., Sholeninov, S.E., and Yurkov, D.I., ADRON-LR instrument for active neutron sensing of the lunar matter composition, *Sol. Syst. Res.,* 2021, vol. 55, pp. 529–536. https://doi.org/10.1134/S0038094621060046

Gómez-Elvira, J., Armiens, C., Castañer, L., Domínguez, M., Genzer, M., Gómez, F., Haberle, R., Harri, A.-M., Jiménez, V., Kahanpää, H., and 29 co-authors, REMS: The environmental sensor suite for the Mars Science Laboratory rover, *Space Sci. Rev.,* 2012, vol. 170, pp. 583–640. https://doi.org/10.1007/s11214-012-9921-1

Gudkova, T.V., Lognonne, P., Zharkov, V.N., and Raevsky, S.N., On the scientific aims of the MISS seismic experiment, *Sol. Syst. Res.,* 2014, vol. 48, pp. 11–12. https://doi.org/10.1134/S0038094614010043

Guzewich, S.D., Fedorova, A.A., Kahre, M.A., and Toigo, A.D., Studies of the 2018/Mars year 34 planet-encircling dust storm, *J. Geophys. Res.: Planets,* 2020, vol. 125, p. e06700. https://doi.org/10.1029/2020JE006700

Harri, A.-M., Linkin, V., Polkko, J., Marov, M., Pommereau, J.-P., Lipatov, A., Siili, T., Manuilov, K., Lebedev, V., Lehto, A., and 10 co-authors, Meteorological observations on Martian surface: Met-packages of Mars-96 small stations and penetrators, *Planet. Space Sci.,* 1998, vol. 46, pp. 779–793. https://doi.org/10.1016/S0032-0633(98)00012-9

Harri, A.-M., Pichkadze, K., Zeleny, L., Vazquez, L., Schmidt, W., Alexashkin, S., Korablev, O., Guerrero, H., Heilimo, J., Uspensky, M., and 22 co-authors, The MetNet vehicle: A lander to deploy environmental stations for local and global investigations of Mars, *Geophys. Instr., Method and Data Syst.,* 2017, vol. 6, pp. 103–124. https://doi.org/10.5194/gi-6-103-2017

Hartogh, P., Medvedev, A.S., Kuroda, T., Saito, R., Villanueva, G., Feofilov, A.G., Kutepov, A.A., and Berger, U., Description and climatology of a new general circulation model of the Martian atmosphere, *J. Geophys. Res.: Planets,* 2005, vol. 110, p. E11008. https://doi.org/10.1029/2005JE002498

Hassler, D.M., Zeitlin, C., Wimmer-Schweingruber, R.F., Böttcher, S., Martin, C., Andrews, J., Bohm, E., Brinza, D.E., Bullock, M.A., Burmeister, S., and 15 co-authors, The Radiation Assessment Detector (RAD) investigation, *Space Sci. Rev.,* 2012, vol. 170, pp. 503–558. https://doi.org/10.1007/s11214-012-9913-1

Hassler, D.M., Zeitlin, C., Wimmer-Schweingruber, R.F., Ehresmann, B., Rafkin, S., Eigenbrode, J.L., Brinza, D.E., Weigle, G., Bottcher, S., Böhm, E., and 438 co-au-

thors, Mars' surface radiation environment measured with the Mars Science Laboratory's *Curiosity* Rover, *Science,* 2014, vol. 343, no. 6169, p. 1244797. https://doi.org/10.1126/science.1244797

Hess, S.L., Ryan, J.A., Tillman, J.E., Henry, R.M., and Leovy, C.B., The annual cycle of pressure on Mars measured by *Viking* landers 1 and 2, *Geophys. Res. Lett.,* 1980, vol. 7, pp. 197–200. https://doi.org/10.1029/GL007i003p00197

Hofer, L., Wurz, P., Buch, A., Cabane, M., Coll, P., Coscia, D., Gerasimov, M., Lasi, D., Sapgir, A., Szopa, C., and Tulej, M., Prototype of the gas chromatograph-mass spectrometer to investigate volatile species in the lunar soil for the *Luna-Resurs* mission, *Planet. Space Sci.,* 2015, vol. 111, pp. 126–133. https://doi.org/10.1029/GL007i003p00197

Holstein-Rathlou, C., Maue, A., and Withers, P., Atmospheric studies from the Mars Science Laboratory entry, descent and landing atmospheric structure reconstruction, *Planet. Space Sci.,* 2016, vol. 120, pp. 15–23. https://doi.org/10.1016/j.pss.2015.10.015

Huang, Q., Schmerr, N.C., King, S.D., and Banerdt, W.B., Seismic detection of a deep mantle discontinuity within Mars by InSight, *Proc. Natl. Acad. Sci. U.S.A.,* 2022, vol. 119, p. e2204474119. . https://doi.org/10.1073/pnas.2204474119

Ivanov, M.A., Slyuta, E.N., Grishakina, E.A., and Dmitrovskii, A.A., Geomorphological analysis of *ExoMars* candidate landing site Oxia Planum, *Sol. Syst. Res.,* 2020, vol. 54, no. 1, pp. 1–14. https://doi.org/10.1134/S0038094620010050

Jakosky, B.M., Zent, A.P., and Zurek, R.W., The Mars water cycle: Determining the role of exchange with the regolith, *Icarus,* 1997, vol. 130, pp. 87–95. https://doi.org/10.1006/Icarus.1997.5799

Jimenez-Martín, J., García Menéndez, E., Gonzalez-Guerrer Bartolomé, M., Martinez-Oter, J., Apéstigue-Palacio, V., de Mingo, J.R., Rivas, J., Serrano, F., Montalvo, S., García-Llases, A., and Arruego, I., Solar Irradiance Sensor of RDM ExoMars 2022 calibration, *Proc. SPIE,* 2023, vol. 12777, p. 1277774. https://doi.org/10.1117/12.2691378

Johnson, C.L., Mittelholz, A., Langlais, B., Russell, C.T., Ansan, V., Banfield, D., Chi, P.J., Fillingim, M.O., Forget, F., Haviland, H.F., and 14 co-authors, Crustal and time-varying magnetic fields at the *InSight* landing site on Mars, *Nat. Geosci.,* 2020, vol. 13, pp. 199–204. https://doi.org/10.1038/s41561-020-0537-x

Kahre, M., Murphy, J., Newman, C., Wilson, R., Cantor, B., Lemmon, M., and Wolff, M., The Mars dust cycle, in *The Atmosphere and Climate of Mars,* Haberle, R., Clancy, R., Forget, F., Smith, M., and Zurek, R., Eds., Cambridge: Cambridge Univ. Press, 2017, pp. 295–337. https://doi.org/10.1017/9781139060172.010

Kahre, M.A., Haberle, R.M., Wilson, R.J., Urata, R.A., Steakley, K.E., Brecht, A.S., Bertrand, T., Kling, A., Batterson, C.M., Hartwick, V., Harman, C.E., and Gkouvelis, L., The NASA Ames legacy Mars global climate model: Radiation code error correction and new baseline water cycle simulation, *Icarus,* 2023, vol. 400, p. 115561. https://doi.org/10.1016/j.Icarus.2023.115561

Karlgaard, C.D., Korzun, A.M., Schoenenberger, M., Bonfiglio, E.P., Kass, D.M., and Grover, M.R., Mars insight entry, descent, and landing trajectory and atmosphere reconstruction, *J. Spacecr. Rockets,* 2021, vol. 58, pp. 865–878. https://doi.org/10.2514/1.A34913

Karlgaard, C.D., Schoenenberger, M., Dutta, S., and Way, D.W., Mars entry, descent, and landing instrumentation 2 trajectory, aerodynamics, and atmosphere reconstruction, *J. Spacecr. Rockets,* 2023, vol. 60, pp. 199–214.

Kawamura, T., Clinton, J.F., Zenhausern, G., Ceylan, S., Horleston, A.C., Dahmen, N.L., Duran, C., Kim, D., Plasman, M., Stahler, S.C., and 8 co-authors, S1222a—the largest Marsquake detected by *InSight, Geophys. Res. Lett.,* 2023, vol. 50, p. e2022GL101543. https://doi.org/10.1029/2022GL101543

Khorkin, V.S., Fedorova, A.A., Dobrolenskiy, Y.S., Korablev, O.I., Vyazovetskiy, N.A., Dzyuban, I.A., Sapgir, A.G., Titov, A.Yu., Toledo, D., Pommereau, J.-P., and Rannou, P., *ExoMars-2022* mission ODS instrument: Modeling and ground field measurements, *Sol. Syst. Res.,* 2023, vol. 57, pp. 324–335. https://doi.org/10.1134/S0038094623040056

Knapmeyer-Endrun, B., Panning, M.P., Bissig, F., Rakshit, J., Khan, A., Kim, D., Lekic, V., Tauzin, B., Tharimena, S., Plasman, M., and 29 co-authors, Thickness and structure of the Martian crust from *InSight* seismic data, *Science,* 2021, vol. 373, no. 6553, pp. 438–443. https://doi.org/10.1126/science.abf8966

Knutsen, E.W., Montmessin, F., Verdier, L., Lacombe, G., Lefevre, F., Ferron, S., Giuranna, M., Wolkenberg, P., Fedorova, A., Trokhimovskiy, A., and Korablev, O., Water vapor on Mars: A refined climatology and constraints on the near-surface concentration enabled by synergistic retrievals, *J. Geophys. Res.: Planets,* 2022, vol. 127, p. e07252. https://doi.org/10.1029/2022JE007252

Kok, J.F. and Renno, N.O., Electrification of wind-blown sand on Mars and its implications for atmospheric chemistry, *Geophys. Res. Lett.*, 2009, vol. 36, no. 5, p. L05202. https://doi.org/10.1029/2008GL036691

Kolmasova, I., Santolik, O., and Skalsky, A., Anticipated plasma wave measurement onboard *ExoMars 2020* surface platform, *Proc. 8th Int. Workshop on Planets, Solar and Heliospheric Radio Emissions, Graz, Austria, October 25–27, 2016,* 2017, p. 487. https://doi.org/10.1553/PRE8s487

Konopliv, A.S., Park, R.S., and Folkner, W.M., An improved JPL Mars gravity field and orientation from Mars orbiter and lander tracking data, *Icarus,* 2016, vol. 274, pp. 253–260. https://doi.org/10.1016/j.icarus.2016.02.052

Konopliv, A.S., Park, R.S., Rivoldini, A., and Baland, R.-M., Le Maistre, S., Van Hoolst, T., Yseboodt, M., and Dehant, V., Detection of the Chandler wobble of Mars from orbiting spacecraft, *Geophys. Res. Lett.,* 2020, vol. 47, p. e90568. https://doi.org/10.1029/2020GL090568

Korablev, O., Montmessin, F., Trokhimovskiy, A., Fedorova, A.A., Shakun, A.V., Grigoriev, A.V., Moshkin, B.E.,

Ignatiev, N.I., Forget, F., Lefèvre, F., and 64 co-authors, The Atmospheric Chemistry Suite (ACS) of three spectrometers for the *ExoMars 2016* Trace Gas Orbiter, *Space Sci. Rev.,* 2018, vol. 214, p. 7. https://doi.org/10.1007/s11214-017-0437-6

Kuchynka, P., Folkner, W.M., Konopliv, A.S., Parker, T.J., Park, R.S., Le Maistre, S., and Dehant, V., New constraints on Mars rotation determined from radiometric tracking of the *Opportunity* Mars exploration rover, *Icarus,* 2014, vol. 229, pp. 340–347. https://doi.org/10.1016/j.icarus.2013.11.015

Kurgansky, M.V., Statistical distribution of atmospheric dust devils on Earth and Mars, *Boundary-Layer Meteorol.,* 1993, vol. 63, pp. 65–96., 2022, vol. 184, pp. 381–400. https://doi.org/10.1007/s10546-022-00713-w

Langlais, B., Thébault, E., Houliez, A., and Purucker, M.E., A new model of the crustal magnetic field of Mars using MGS and MAVEN, *J. Geophys. Res.: Planets,* 2019, vol. 124, pp. 1542–1569.

Le Maistre, S., Péters, M.-J., Marty, J.-C., and Dehant, V., On the impact of the operational and technical characteristics of the LaRa experiment on the determination of Mars' nutation, *Planet Space Sci.,* 2020, vol. 180, p. 104766. https://doi.org/10.1016/j.pss.2019.104766

Lefèvre, F., Trokhimovskiy, A., Fedorova, A., Baggio, L., Lacombe, G., Määttänen, A., Bertaux, J.-L., Forget, F., Millour, E., Venot, O., Bénilan, Y., Korablev, O., and Montmessin, F., Relationship between the ozone and water vapor columns on Mars as observed by SPICAM and calculated by a Global Climate Model, *J. Geophys. Res.: Planets,* 2021, vol. 126, p. e06838. https://doi.org/10.1029/2021JE006838

Linkin, V., Harri, A.-M., Lipatov, A., Belostotskaja, K., Derbunovich, B., Ekonomov, A., Khloustova, L., Kremnev, R., Makarov, V., Martinov, B., and 11 co-authors, A sophisticated lander for scientific exploration of Mars: Scientific objectives and implementation of the *Mars-96* small station, *Planet. Space Sci.,* 1998, vol. 46, pp. 717–737. https://doi.org/10.1016/S0032-0633(98)00008-7

Lipatov, A.N., Ekonomov, A.P., Makarov, V.S., Lesnykh, V.A., Goretov, V.A., Zakharkin, G.V., Zaitsev, M.A., Khlyustova, L.I., and Antonenko, S.A., Accelerometers of the meteorological complex for the study of the upper atmosphere of Mars, *Sol. Syst. Res.,* 2023a, vol. 57, no. 4, pp. 349–357. https://doi.org/10.1134/S0038094623040081

Lipatov, A.N., Ekonomov, A.P., Makarov, V.S., Lesnykh, V.A., Goretov, V.A., Zakharkin, G.V., Zaitsev, M.A., Khlyustova, L.I., and Antonenko, S.A., Temperature and pressure sensors of the meteorological complex for the study of the Mars's atmosphere, *Sol. Syst. Res.,* 2023b, vol. 57, no. 4, pp. 336–348. https://doi.org/10.1134/S003809462304007X

Lipatov, A.N., Lyash, A.N., Ekonomov, A.P., Makarov, V.S., Lesnykh, V.A., Goretov, V.A., Zakharkin, G.V., Khlyustova, L.I., Antonenko, S.A., Rodionov, D.S., and Korablev, O.I., LIDAR for investigation of the Martian atmosphere from the surface, *Sol. Syst. Res.,* 2023c, vol. 57, no. 4, pp. 358–372. https://doi.org/10.1134/S0038094623040093

Liu, J., Li, C., Zhang, R., Rao, W., Cui, X., Geng, Y., Jia, Y., Huang, H., Ren, X., Yan, W., and 13 co-authors, Geomorphic contexts and science focus of the Zhurong landing site on Mars, *Nat. Astron.,* 2022, vol. 6, pp. 65–71. https://doi.org/10.1038/s41550-021-01519-5

Lognonné, P., Zharkov, V.N., Karczewski, J.F., Romanowicz, B., Menvielle, M., Poupinet, G., Brient, B., Cavoit, C., Desautez, A., Dole, B., et al., The seismic optimism experiment, *Planet. Space Sci.,* 1998, vol. 46, pp. 739–747. https://doi.org/10.1016/S0032-0633(98)00009-9

Lognonné, P., Giardini, D., Banerdt, B., Gagnepain-Beyneix, J., Mocquet, A., Spohn, T., Karczewski, J.F., Schibler, P., Cacho, S., Pike, W.T., and 5 co-authors, The NetLander very broad band seismometer, *Planet. Space Sci.,* 2000, vol. 48, pp. 1289–1302. https://doi.org/10.1016/S0032-0633(00)00110-0

Lognonne, P., Banerdt, W.B., Giardini, D., Pike, W.T., Christensen, U., Laudet, P., de Raucourt, S., Zweifel, P., Calcutt, S., Bierwirth, M., and 161 co-authors, SEIS: *InSight*'s seismic experiment for internal structure of Mars, *Space Sci. Rev.,* 2019, vol. 215, p. 12. https://doi.org/10.1007/s11214-018-0574-6

Magalhães, J.A., Schofield, J.T., and Seiff, A., Results of the Mars pathfinder atmospheric structure investigation, *J. Geophys. Res.: Planets,* 1999, vol. 104, pp. 8943–8955. https://doi.org/10.1029/1998JE900041

Mahaffy, P.R., Webster, C.R., Atreya, S.K., Franz, H., Wong, M., Conrad, P.G., Harpold, D., Jones, J.J., Leshin, L.A., Manning, H., and 439 co-authors, Abundance and isotopic composition of gases in the Martian atmosphere from the *Curiosity* rover, *Science,* 2013, vol. 341, no. 6143, pp. 263–266. https://doi.org/10.1126/science.1237966

Malakhov, A.V., Mitrofanov, I.G., Golovin, D.V., Litvak, M.L., Sanin, A.B., Djachkova, M.V., and Lukyanov, N.V., High resolution map of water in the Martian regolith observed by FREND neutron telescope onboard *ExoMars* TGO, *J. Geophys. Res.: Planets,* 2022, vol. 127, p. e07258. https://doi.org/10.1029/2022JE007258

Manukin, A.B., Gorshkov, A.N., and Shlyk, A.F., GRAS-F seismogravimeter for measuring gravity-inertial fields on the surface of Phobos, *Sol. Syst. Res.,* 2010, vol. 44, pp. 417–422. https://doi.org/10.1134/S0038094610050096

Manukin, A.B., Kazantseva, O.S., Kalinnikov, I.I., Matyunin, V.P., Sayakina, N.F., Ton'shev, A.K., and Chernogorova, N.A., A seismometer for observations on Mars, *Cosmic Res.,* 2021, vol. 59, pp. 366–375. https://doi.org/10.1134/S0010952521050087

Martin, R.L. and Kok, J.F., Wind-invariant saltation heights imply linear scaling of aeolian saltation flux with shear stress, *Sci. Adv.,* 2017, vol. 3, p. e1602569. https://doi.org/10.1126/sciadv.1602569

Martín-Torres, J., Zorzano, M.-P., Soria-Salinas, Á., Nazarious, M.I., Konatham, S., Mathanlal, T., Ramachandran, A.V., Ramírez-Luque, J.-A., and Mantas-Nakhai, R., The HABIT (HabitAbility: Brine Irradiation and Temperature) environmental instrument for the *ExoMars 2022* Surface Platform, *Planet. Space Sci.,*

2020, vol. 190, p. 104968.
https://doi.org/10.1016/j.pss.2020.104968

Mitrofanov, I.G., Litvak, M.L., Varenikov, A.B., Barmakov, Y.N., Behar, A., Bobrovnitsky, Y.I., Bogolubov, E.P., Boynton, W.V., Harshman, K., Kan, E., and 13 co-authors, Dynamic Albedo of Neutrons (DAN) experiment onboard NASA's Mars Science Laboratory, *Space Sci. Rev.,* 2012, vol. 170, pp. 559–582.
https://doi.org/10.1007/s11214-012-9924-y

Mitrofanov, I.G., Litvak, M.L., Nikiforov, S.Y., Jun, I., Bobrovnitsky, Y.I., Golovin, D.V., Grebennikov, A.S., Fedosov, F.S., Kozyrev, A.S., Lisov, D.I., and 8 co-authors, The ADRON-RM instrument onboard the *ExoMars* rover, *Astrobiology,* 2017, vol. 17, pp. 585–594.
https://doi.org/10.1089/ast.2016.1566

Mitrofanov, I., Malakhov, A., Bakhtin, B., Golovin, D., Kozyrev, A., Litvak, M., Mokrousov, M., Sanin, A., Tretyakov, V., Vostrukhin, A., and 16 co-authors, Fine Resolution Epithermal Neutron Detector (FREND) onboard the *ExoMars* Trace Gas Orbiter, *Space Sci. Rev.,* 2018, vol. 214, p. 86.
https://doi.org/10.1007/s11214-018-0522-5

Mitrofanov, I.G., Kozyrev, A.S., Lisov, D.I., Litvak, M.L., Malakhov, A.A., Mokrousov, M.I., Benkhoff, J., Owens, A., Schulz, R., and Quarati, F., The Mercury Gamma-Ray and Neutron Spectrometer (MGNS) onboard the Mercury Planetary Orbiter of the *BepiColombo* mission: Design updates and first measurements in space, *Space Sci. Rev.,* 2021, vol. 217, p. 67.
https://doi.org/10.1007/s11214-021-00842-7

Mitrofanov, I., Malakhov, A., Djachkova, M., Golovin, D., Litvak, M., Mokrousov, M., Sanin, A., Svedhem, H., and Zelenyi, L., The evidence for unusually high hydrogen abundances in the central part of Valles Marineris on Mars, *Icarus,* 2022a, vol. 374, p. 114805.
https://doi.org/10.1016/j.Icarusus.2021.114805

Mitrofanov, I.G., Nikiforov, S.Y., Djachkova, M.V., Lisov, D.I., Litvak, M.L., Sanin, A.B., and Vasavada, A.R., Water and chlorine in the Martian subsurface along the traverse of NASA's *Curiosity* rover: 1. DAN measurement profiles along the traverse, *J. Geophys. Res.: Planets,* 2022b, vol. 127, p. e2022JE007327.
https://doi.org/10.1029/2022JE007327

Mittelholz, A., Johnson, C.L., Thorne, S.N., Joy, S., Barrett, E., Fillingim, M.O., Forget, F., Langlais, B., Russell, C.T., Spiga, A., Smrekar, S., and Banerdt, W.B., The origin of observed magnetic variability for a sol on Mars from *InSight, J. Geophys. Res.: Planets,* 2020, vol. 125, no. 9, p. e2020JE006505.
https://doi.org/10.1029/2020JE006505

Mokrousov, M.I., Golovin, D.V., Mitrofanov, I.G., Anikin, A.A., Kozyrev, A.S., Litvak, M.L., Malakhov, A.V., Nikiforov, S.Y., Pekov, A.N., Sanin, A.B., and Tretyakov, V.I., ADRON: Active Spectrometer of Neutron and Gamma Radiation of the Moon and Mars, *Phys. Particles Nuclei Lett.,* 2022, vol. 19, pp. 744–764.
https://doi.org/10.1134/S1547477122060164

Montabone, L., Forget, F., Millour, E., Wilson, R.J., Lewis, S.R., Cantor, B., Kass, D., Kleinbohl, A., Lemmon, M.T., Smith, M.D., and Wolff, M.J., Eight-year climatology of dust optical depth on Mars, *Icarus,* 2015, vol. 251, pp. 65–95.

Montmessin, F., Smith, M., Langevin, Y., Mellon, M., and Fedorova, A., The water cycle, in *The Atmosphere and Climate of Mars,* Haberle, R., Clancy, R., Forget, F., Smith, M., and Zurek, R., Eds., Cambridge: Cambridge Univ. Press, 2017.
https://doi.org/10.1017/9781139060172.011

Moskatin'ev, I.V., Ivanov, A.S., Aleksashkin, S.N., and Ostreshko, B.A., *ExoMars-2022* spacecraft, in *Rossiiskii segment mezhdunarodnoi kosmicheskoi ekspeditsii "EkzoMars-2022"* (Russian Segment of the International Space Mission *Exomars-2022*), Efanov, V.V. and Karchaev, Kh.Zh., Eds., Khimki: NPO im. S.A. Lavochkina, 2020a, vol. 1, pp. 52–56.

Moskatin'ev, I.V., Ivanov, A.S., Aleksashkin, S.N., and Ostreshko, B.A., *ExoMars-2022* landing module, in *Rossiiskii segment mezhdunarodnoi kosmicheskoi ekspeditsii "EkzoMars-2022"* (Russian Segment of the International Space Mission *Exomars-2022*), Efanov, V.V. and Karchaev, Kh.Zh., Eds., Khimki: NPO im. S.A. Lavochkina, 2020a, vol. 1, pp. 100–111.

Musiolik, G., Kruss, M., Demirci, T., Schrinski, B., Teiser, J., Daerden, F., Smith, M.D., Neary, L., and Wurm, G., Saltation under Martian gravity and its influence on the global dust distribution, *Icarus,* 2018, vol. 306, pp. 25–31.
https://doi.org/10.1016/j.Icarusus.2018.01.007

Navarro, T., Madeleine, J.-B., Forget, F., Spiga, A., Millour, E., Montmessin, F., and Maattanen, A., Global climate modeling of the Martian water cycle with improved microphysics and radiatively active water ice clouds, *J. Geophys. Res.: Planets,* 2014, vol. 119, pp. 1479–1495.
https://doi.org/10.1002/2013JE004550

Neakrase, L.D.V., Balme, M.R., Esposito, F., Kelling, T., Klose, M., Kok, J.F., Marticorena, B., Merrison, J., Patel, M., and Wurm, G., Particle lifting processes in dust devils, *Space Sci. Rev.,* 2016, vol. 203, pp. 347–376.
https://doi.org/10.1007/s11214-016-0296-6

Neary, L. and Daerden, F., The GEM-Mars general circulation model for Mars: Description and evaluation, *Icarus,* 2018, vol. 300, pp. 458–476.
https://doi.org/10.1016/j.Icarus.2017.09.028

Newman, C.E. and Richardson, M.I., The impact of surface dust source exhaustion on the Martian dust cycle, dust storms and interannual variability, as simulated by the MarsWRF General Circulation Model, *Icarus,* 2015, vol. 257, pp. 47–87.
https://doi.org/10.1016/j.Icarusus.2015.03.030

Pavlov, A.K., Shelegedin, V.N., Vdovina, M.A., and Pavlov, A.A., Growth of microorganisms in Martian-like shallow subsurface conditions: Laboratory modelling, *Int. J. Astrobiol.,* 2010, vol. 9, pp. 51–58.
https://doi.org/10.1017/S1473550409990371

Péters, M.-J., Le Maistre, S., Yseboodt, M., Marty, J.-C., Rivoldini, A., Van Hoolst, T., and Dehant, V., LaRa after RISE: Expected improvement in the Mars rotation and interior models, *Planet. Space Sci.,* 2020, vol. 180, no. 4, p. 104745.
https://doi.org/10.1016/j.pss.2019.104745

Petrosyan, A., Galperin, B., Larsen, S.E., Lewis, S.R., Maattanen, A., Read, P.L., Renno, N., Rogberg, L.P.H.T., Savijarvi, H., Siili, T., Spiga, A., Toigo, A., and Vazquez, L., The Martian atmospheric boundary layer, *Rev. Geophys.,* 2011, vol. 49, no. 3,

p. RG3005.
https://doi.org/10.1029/2010RG000351

Read, P., Galperin, B., Larsen, S., Lewis, S.R., Maattanen, A., Petrosyan, A., Renno, N., Savijärvi, H., Siili, T., and Spiga, A., The Martian planetary boundary layer, in *The Atmosphere and Climate of Mars,* Haberle, R., Clancy, R., Forget, F., Smith, M., and Zurek, R., Eds., Cambridge: Cambridge Univ. Press, 2017, pp. 172–202.
https://doi.org/10.1017/9781139060172.007

Renno, N.O., Wong, A.-S., Atreya, S.K., de Pater, I., and Roos-Serote, M., Electrical discharges and broadband radio emission by Martian dust devils and dust storms, *Geophys. Res. Lett.,* 2003, vol. 30, p. 2140.
https://doi.org/10.1029/2003GL017879

Rodin, A., Vinogradov, I., Zenevich, S., Spiridonov, M., Gazizov, I., Kazakov, V., Meshcherinov, V., Golovin, I., Kozlova, T., Lebedev, Y., and 11 co-authors, Martian Multichannel Diode Laser Spectrometer (M-DLS) for in-situ atmospheric composition measurements on Mars onboard *ExoMars-2022* landing platform, *Appl. Sci.,* 2020, vol. 10, no. 24, p. 8805.
https://doi.org/10.3390/app10248805

Rodriguez-Manfredi, J.A., de la Torre Juárez, M., Alonso, A., Apéstigue, V., Arruego, I., Atienza, T., Banfield, D., Boland, J., Carrera, M.A., Castañer, L., and 76 co-authors, The Mars Environmental Dynamics Analyzer, MEDA. A suite of environmental sensors for the Mars 2020 mission, *Space Sci. Rev.,* 2021, vol. 217, p. 48.
https://doi.org/10.1007/s11214-021-00816-9

Sagan, C. and Bagnold, R.A., Fluid transport on Earth and Aeolian transport on Mars, *Icarus,* 1975, vol. 26, pp. 209–218.
https://doi.org/10.1016/0019-1035(75)90080-9

Seiff, A. and Kirk, D.B., Structure of the atmosphere of Mars in summer at mid-latitudes, *J. Geophys. Res.,* 1977, vol. 82, pp. 4364–4378.
https://doi.org/10.1029/JS082i028p04364

Seiff, A., Tillman, J.E., Murphy, J.R., Schofield, J.T., Crisp, D., Jeffrey, R.B., LaBaw, C., Mahoney, C., Mihalov, J.D., Wilson, G.R., and Haberle, R., The atmosphere structure and meteorology instrument on the Mars pathfinder lander, *J. Geophys. Res.: Planets,* 1997, vol. 102, pp. 4045–4056.
https://doi.org/10.1029/96JE03320

Semkova, J., Dachev, T., Matviichuk, Y., Koleva, R., Tomov, B., Baynov, P., Petrov, V., Nguyen, V., Siegrist, M., Chene, J., d'Uston, C., and Cotin, F., Dosimetric investigations on *Mars-96* mission, *Adv. Space Res.*, 1994, vol. 14, pp. 707–710.
https://doi.org/10.1016/0273-1177(94)90530-4

Semkova, J., Koleva, R., Benghin, V., Dachev, T., Matviichuk, Y., Tomov, B., Krastev, K., Maltchev, S., Dimitrov, P., Bankov, N., and 10 co-authors, Results from radiation environment measurements aboard *ExoMars* Trace Gas Orbiter in Mars science orbit in May 2018–December 2019, *Icarus,* 2021, vol. 361, p. 114264.
https://doi.org/10.1016/j.Icarusus.2020.114264

Shakun, A., Korablev, O., Moshkin, B., Grigoriev, A., Ignatiev, N., Maslov, I., Sazonov, O., Patsaev, D., Kungurov, A., Santos-Skripko, A., and 7 co-authors, Fourier transform spectrometers for remote sensing of planetary atmospheres and surfaces, *CEAS Space J.,* 2017, vol. 9, pp. 399–409.
https://doi.org/10.1007/s12567-017-0176-2

Shakun, A., Ignatiev, N., Luginin, M., Grigoriev, A., Moshkin, B., Grassi, D., Arnold, G., Maturilli, A., Kungurov, A., Makarov, V., and 11 co-authors, ACS/TIRVIM: Calibration and first results, *Proc. SPIE,* 2018, vol. 10765, p. 107650E.
https://doi.org/10.1117/12.2322163

Shakun, A., Kungurov, A., Sazonov, O., Stupin, I., Arnold, G., Grigoriev, A., and Korablev, O., Two-coordinate pointing and tracking system for an infrared Fourier-transform spectrometer, *Proc. SPIE,* 2019a, vol. 11128, p. 111280H.
https://doi.org/10.1117/12.2535444

Shakun, A., Santos-Skripko, A., Sazonov, O., Maslov, I., Ignatiev, N., Stupin, I., Arnold, G., Grigoriev, A., and Korablev, O., Interferometer with single-axis robot: Design, alignment and performance, *Proc. SPIE,* 2019b, vol. 11128, p. 111280G.
https://doi.org/10.1117/12.2535436

Smith, M.D., Wolff, M.J., Spanovich, N., Ghosh, A., Banfield, D., Christensen, P.R., Landis, G.A., and Squyres, S.W., One Martian year of atmospheric observations using MER Mini-TES, *J. Geophys. Res.: Planets,* 2006, vol. 111, p. E12S13.
https://doi.org/10.1029/2006JE002770

Smith, M., Bougher, S., Encrenaz, T., Forget, F., and Kleinböhl, A., Thermal structure and composition, in *The Atmosphere and Climate of Mars,* Haberle, R., Clancy, R., Forget, F., Smith, M., and Zurek, R., Eds., Cambridge: Cambridge Univ. Press, 2017, pp. 42–75.
https://doi.org/10.1017/9781139060172.004

Smith, M.D., Daerden, F., Neary, L., Khayat, A.S.J., Holmes, J.A., Patel, M.R., Villanueva, G., Liuzzi, G., Thomas, I.R., Ristic, B., Bellucci, G., Lopez-Moreno, J.J., and Vandaele, A.C., The climatology of carbon monoxide on Mars as observed by NOMAD nadir-geometry observations, *Icarus,* 2021, vol. 362, p. 114404.
https://doi.org/10.1016/j.icarus.2021.114404

Soria-Salinas, Á., Zorzano, M.-P., Mantas-Nakhai, R., and Martín-Torres, J., Wind retrieval from temperature measurements from the Rover Environmental Monitoring Station/Mars Science Laboratory, *Icarus*, 2020, vol. 346, p. 113785.
https://doi.org/10.1016/j.Icarus.2020.113785

Spiga, A., Banfield, D., Teanby, N.A., Forget, F., Lucas, A., Kenda, B., Rodriguez Manfredi J.A., Widmer-Schnidrig, R., Murdoch, N., Lemmon, M.T., and 27 co-authors, Atmospheric science with *InSight, Space Sci. Rev.,* 2018, vol. 214, p. 109.
https://doi.org/10.1007/s11214-018-0543-0

Stähler, S.C., Khan, A., Banerdt, W.B., Lognonne, P., Giardini, D., Ceylan, S., Drilleau, M., Duran, A.C., Garcia, R.F., Huang, Q., and 31 co-authors, Seismic detection of the Martian core, *Science,* 2021, vol. 373, pp. 443–448.
https://doi.org/10.1126/science.abi7730

Taylor, P.A., Catling, D.C., Daly, M., Dickinson, C.S., Gunnlaugsson, H.P., Harri, A.-M., and Lange, C.F., Temperature, pressure, and wind instrumentation in the phoenix meteorological package, *J. Geophys. Res.,* 2008, vol. 113, p. E00A10.
https://doi.org/10.1029/2007JE003015

Todd, J.F.J., Barber, S.J., Wright, I.P., Morgan, G.H., Morse, A.D., Sheridan, S., Leese, M.R., Maynard, J., Evans, S.T., Pillinger, C.T., and 7 co-authors, Ion trap mass spectrometry on a comet nucleus: The Ptolemy instrument and the *Rosetta* space mission, *J. Mass Spectrometry,* 2007, vol. 42, pp. 1–10. https://doi.org/10.1002/jms.1147

Toigo, A.D., Richardson, M.I., Wilson, R.J., Wang, H., and Ingersoll, A.P., A first look at dust lifting and dust storms near the south pole of Mars with a mesoscale model, *J. Geophys. Res.: Planets,* 2002, vol. 107, p. 5050. https://doi.org/10.1029/2001JE001592

Toledo, D., Rannou, P., Pommereau, J.-P., Sarkissian, A., and Foujols, T., Measurement of aerosol optical depth and sub-visual cloud detection using the optical depth sensor (ODS), *Atmos. Meas. Tech.,* 2016, vol. 9, pp. 455–467. https://doi.org/10.5194/amt-9-455-2016

Toledo, D., Arruego, I., Apéstigue, V., Jimenez, J.J., Gómez, L., Yela, M., Rannou, P., and Pommereau, J.-P., Measurement of dust optical depth using the solar irradiance sensor (SIS) onboard the *ExoMars 2016* EDM, *Planet. Space Sci.,* 2017, vol. 138, pp. 33–43. https://doi.org/10.1016/j.pss.2017.01.015

Vago, J., Witasse, O., Svedhem, H., Baglioni, P., Haldemann, A., Gianfiglio, G., Blancquaert, T., McCoy, D., and de Groot, R., ESA ExoMars program: The next step in exploring Mars, *Sol. Syst. Res.,* 2015a, vol. 49, pp. 518–528. https://doi.org/10.1134/S0038094615070199

Vago, J.L., Lorenzoni, L., Calantropio, F., and Zashchirinskiy, A.M., Selecting a landing site for the ExoMars 2018 mission, *Sol. Syst. Res.,* 2015b, vol. 49, pp. 538–542. https://doi.org/10.1134/S0038094615070205

Vago, J.L. and Westall, F., Pasteur Instrument Teams, Landing Site Selection Working Group, Other Contributors, Coates, A.J., Jaumann, R., Korablev, O., Ciarletti, V., Mitrofanov, I., and 66 co-authors, Habitability on early Mars and the search for biosignatures with the *ExoMars* rover, *Astrobiology*, 2017, vol. 17, pp. 471–510. https://doi.org/10.1089/ast.2016.1533

Webster, C.R., Mahaffy, P.R., Flesch, G.J., Niles, P.B., Jones, J.H., Leshin, L.A., Atreya, S.K., Stern, J.C., Christensen, L.E., Owen, T., and 4 co-authors, Isotope ratios of H, C, and O in CO_2 and H_2O of the Martian atmosphere, *Science,* 2013, vol. 341, no. 6143, pp. 260–263. https://doi.org/10.1126/science.1237961

Wilson, R.J. and Hamilton, K., Comprehensive model simulation of thermal tides in the Martian atmosphere, *J. Atmos. Sci.,* 1996, vol. 53, no. 9, pp. 1290–1326. https://doi.org/10.1175/1520-0469(1996)053<1290CMSOTT>2.0.CO;2

Withers, P. and Smith, M.D., Atmospheric entry profiles from the Mars exploration rovers *Spirit* and *Opportunity, Icarus,* 2006, vol. 185, pp. 133–142. https://doi.org/10.1016/j.icarus.2006.06.013

Wolff, M.J., Smith, M.D., Clancy, R., Spanovich, N., Whitney, B., Lemmon, M.T., Bandfield, J.L., Banfield, D., Ghosh, A., Landis, G., Christensen, P.R., Bell, J.F. III, and Squyres, S.W., Constraints on dust aerosols from the Mars Exploration Rovers using MGS overflights and Mini-TES, *J. Geophys. Res.: Planets,* 2006, vol. 111, p. E12S17. https://doi.org/10.1029/2006je002786

Wolff, M.J., Smith, M.D., Clancy, R.T., Arvidson, R., Kahre, M., Seelos, F. IV, Murchie, S., and Savijärvi, H., Wavelength dependence of dust aerosol single scattering albedo as observed by the Compact Reconnaissance Imaging Spectrometer, *J. Geophys. Res.: Planets,* 2009, vol. 114, p. E00D04. https://doi.org/10.1029/2009JE003350

Wong, M.H., Atreya, S.K., Mahaffy, P.N., Franz, H.B., Malespin, C., Trainer, M.G., Stern, J.C., Conrad, P.G., Manning, H.L.K., Pepin, R.O., and 7 co-authors, Isotopes of nitrogen on Mars: Atmospheric measurements by *Curiosity*'s mass spectrometer, *Geophys. Res. Lett.,* 2013, vol. 40, pp. 6033–6037. https://doi.org/10.1002/2013GL057840

Yoder, C.F. and Standish, E.M., Martian precession and rotation from *Viking* lander range data, *J. Geophys. Res.: Planets,* 1997, vol. 102, pp. 4065–4080. https://doi.org/10.1029/96JE03642

Zakharov, A.V., Dol'nikov, G.G., Kuznetsov, I.A., Lyash, A.N., Dubov, A.E., Afonin, V.V., Bednyakov, S.A., Bychkova, A.S., Grushin, V.A., Dokuchaev, I.V., and 10 co-authors, PmL instrument onboard *Luna-25* lander: Plasma-dust measurements in the surface exosphere, *Sol. Syst. Res.,* 2021, vol. 55, no. 6, pp. 576–587. https://doi.org/10.1134/S0038094621060125

Zakharov, A.V., Dolnikov, G.G., Kuznetsov, I.A., Lyash, A.N., Esposito, F., Molfese, C., Arruego Rodríguez, I., Seran, E., Godefroy, M., and 38 co-authors, Dust complex for studying the dust particle dynamics in the near-surface atmosphere of Mars, *Sol. Syst. Res.,* 2022, vol. 56, no. 6, pp. 351–368. https://doi.org/10.1134/S0038094622060065

Zelenyi, L.M., Korablev, O.I., Rodionov, D.S., Novikov, B.S., Marchenkov, K.I., Andreev, O.N., and Larionov, E.V., Scientific objectives of the scientific equipment of the landing platform of the *ExoMars-2018* mission, *Sol. Syst. Res.,* 2015, vol. 49, pp. 509–517. https://doi.org/10.1134/S0038094615070229

Zharkov, V.N., The internal structure of Mars: A key to understanding the origin of terrestrial planets, *Sol. Syst. Res.,* 1996, vol. 30, pp. 456–465.

Translated by M. Samokhina